

2018-04-01

CRISPR-Cas9 Transfection Optimization and Use in a Forward Genetic Screen to Identify Telomere Length Maintenance Genes

Kelsey Phillips
Brigham Young University

Follow this and additional works at: <https://scholarsarchive.byu.edu/etd>

BYU ScholarsArchive Citation

Phillips, Kelsey, "CRISPR-Cas9 Transfection Optimization and Use in a Forward Genetic Screen to Identify Telomere Length Maintenance Genes" (2018). *All Theses and Dissertations*. 7357.
<https://scholarsarchive.byu.edu/etd/7357>

This Thesis is brought to you for free and open access by BYU ScholarsArchive. It has been accepted for inclusion in All Theses and Dissertations by an authorized administrator of BYU ScholarsArchive. For more information, please contact scholarsarchive@byu.edu, ellen_amatangelo@byu.edu.

CRISPR-Cas9 Transfection Optimization and Use in a Forward Genetic Screen
to Identify Telomere Length Maintenance Genes

Kelsey Phillips

A thesis submitted to the faculty of
Brigham Young University
in partial fulfillment of the requirements for the degree of

Master of Science

Jason M. Hansen, Chair
Jonathan K. Alder
Paul R. Reynolds
Steven M. Johnson

Department of Physiology and Developmental Biology

Brigham Young University

Copyright © 2018 Kelsey Phillips

All Rights Reserved

ABSTRACT

CRISPR-Cas9 Transfection Optimization and use in a Forward Genetic Screen to Identify Telomere Length Maintenance Genes

Kelsey Phillips

Department of Physiology and Developmental Biology, BYU
Master of Science

Mutations in the telomere length maintenance pathway can lead to a spectrum of diseases called telomere syndromes, however, the pathway is not fully understood and there may still be unknown components. We designed a forward genetic screen to identify new genes involved in telomere length maintenance. Of the top ranked genes, ZNF827, a zinc finger protein, is the most promising candidate gene. The possible discovery of a new component involved in telomere length maintenance increases our understanding of the pathway and opens new avenues of research. Recent advances in molecular biology techniques, such as the use of RNA-guided nuclease CRISPR associated protein 9 (Cas9), have made screens like this possible. Cas9 is a nuclease that uses a guide RNA (gRNA) to direct its endonuclease activity. The use of Cas9 has revolutionized the field of genome engineering, providing scientists with more efficient methods to knockout and modify genomes. We sought to optimize CRISPR-Cas9 genome editing to make it as widely accessible as possible. We compared plasmid, ribonucleoprotein (RNP), and RNA only lipid-mediated transfection of CRISPR-Cas9 into cell lines using a novel reporter system to measure genome editing efficiency. All methods were successful to some extent, however, RNP lipofection was the most efficient and has many advantages over other methods. We also found that short homology arms of 30-35bp on donor templates was able to mediate site specific editing. These methods should broaden the accessibility of CRISPR-Cas9 genome editing.

Keywords: CRISPR-Cas9, telomere, telomerase, forward genetic screen, ZNF827

ACKNOWLEDGEMENTS

I would not have been able to accomplish this work without the help of Dr. Jonathan Alder and the guidance and assistance he gave me as I worked on these projects. Members of the Alder lab were also instrumental in this work, specifically, Mitch Garey, Mark Roth, and Kelsey Hirschi helped a significant amount with the research presented in this thesis. I would also like to thank Dr. Jason Hansen for becoming my committee chair and allowing me to transfer into his lab to finish my research. I would also like to acknowledge the other co-authors on the CRISPR-Cas9 optimization paper, namely Dr. Arminda Suli and Ted Piorczynski for the help they were in generating the data for that paper.

I would also like to thank BYU and the Simmons Center for Cancer Research for funding that I received during my degree that helped me to focus on my projects. Also members of my family, specifically my husband, Matt, who supported me and my mother, Amy, and sister, Eliza, who helped with my son, Ellis, so that I could finish this project.

TABLE OF CONTENTS

TITLE PAGE.....	i
ABSTRACT	ii
ACKNOWLEDGEMENTS	iii
TABLE OF CONTENTS	iv
LIST OF TABLES	vi
LIST OF FIGURES	vii
INTRODUCTION	1
MATERIAL AND METHODS.....	7
Plasmid Construction.....	7
Cell Culture and Transfection.....	7
Flow Cytometry and Microscopy.....	8
Genomic DNA Collection, Screening, and Sequencing of Modified Clones.....	9
Donor Template Creation.....	9
Western Blots.....	9
Protein Purification.....	9
In Vitro Transcription and In Vitro Cutting with Cas9.....	10
Hydrogen Peroxide Challenge.....	10
Viral Packaging and Transduction.....	11
Telomerase Repeated Amplification Protocol (TRAP) Assay.....	11
Forward Genetic Screen	11
GeCKO PCR and Deep Sequencing.....	12
Data Analysis.....	12
RESULTS	13
CRISPR-Cas9 Optimization.....	13

RNP Lipofection Showed Highest Efficiency of Knockout	13
Knocking Out Endogenous Genes Using RNP Transfection.....	16
Comparison of Methods for Cas9-mediated Genome Editing Using a Reporter System.....	19
Larger Knock-ins Using a Reporter System.....	22
Forward Genetic Screen for Telomere Length Maintenance Genes.....	24
Knockout of TERT Protects Cells from MT-hTR-AU5 Transduction.....	24
Forward Genetic Screen Identifies ZNF827.....	28
ZNF827 Verification.....	32
DISCUSSION.....	35
REFERENCES.....	40
CURRICULUM VITAE.....	48

LIST OF TABLES

Table 1: Telomere Genes Known to Cause Pulmonary Fibrosis When Mutated.....4

Table 2: Top Positive Ranked Genes from Forward Genetic Screen32

Table S1: Supplemental Table of Primers and Oligionucleotides Used for
Screening and Cloning47

LIST OF FIGURES

Figure 1: Telomerase Holoenzyme and Telomere Related Proteins	2
Figure 2: Cas9 Cutting and Repair.....	5
Figure 3: Comparison of Methods to Introduce Cas9 and Guide RNAs.....	15
Figure 4: RNP Mediated Disruption of Endogenous Genes.....	18
Figure 5: Comparison of Methods for Inserting Exogenous Sequences.....	21
Figure 6: Introduction of Epitope Tags and Fluorescent-Protein Tags Using RNP Transfection.....	23
Figure 7: Knockout of TERT can Protect from MT-hTR-AU5 Infection.....	27
Figure 8: Forward Genetic Screen Experimental Design and Results.....	31
Figure 9: Verification of ZNF827.....	34

INTRODUCTION

Telomeres are long nucleotide repeats that cap the ends of chromosomes and are thought to play a role in molecular aging. Telomere dysfunction has been linked to many degenerative disorders including pulmonary fibrosis (Armanios and Blackburn, 2012; Armanios et al., 2005; Armanios et al., 2007). Incidence of pulmonary fibrosis is increasing worldwide, yet there is still a lack of promising treatment options (Hutchinson et al., 2015; Hutchinson et al., 2014). Further understanding of the role of telomeres in the development and progression of pulmonary fibrosis is necessary for future studies into the molecular causes of the disease as well as possible treatments.

Telomeres protect the ends of chromosomes by binding a group of proteins collectively known as shelterin. The shelterin complex prevents the ends of chromosomes from being seen as double stranded breaks in the DNA and suppresses the DNA damage response (de Lange, 2010; Doksan and de Lange, 2014). The shelterin complex is made up of 6 different proteins: TRF1, TRF2, TIN2, TPP1, POT1, and RAP1 (de Lange, 2005; Lackner et al., 2011)(Figure 1B). The loss of shelterin components results in a DNA damage response and subsequent senescence or apoptosis (Lackner et al., 2011).

With cell replication, telomeres shorten and over successive rounds of cell division eventually reach a critical length and can no longer block the DNA damage response. In this way telomeres function as a biological clock and are thought to play a role in aging and age-related diseases. Telomerase can elongate telomeres to prevent telomere shortening over many cell divisions (Blackburn et al., 1989; Greider and Blackburn, 1985; Schmidt and Cech, 2015). The telomerase enzyme is composed of a catalytic reverse transcriptase, TERT, and an RNA template, telomerase RNA (TR) (Figure 1A). TR contains the complimentary sequence to the

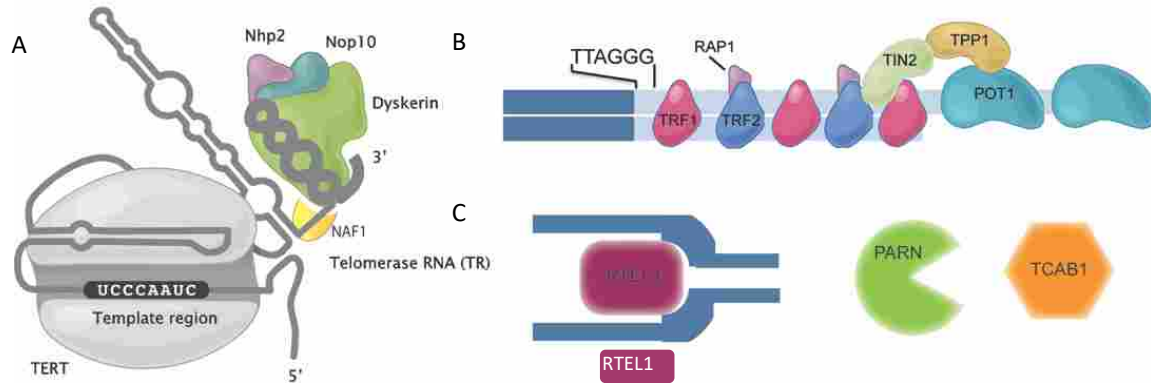


Figure 1: Telomerase Holoenzyme and Telomere Related Proteins. A) Telomerase holoenzyme including the protein component TERT and RNA component TR as well as Nhp2, Nop10, Dyskerin, and NAF1. B) Shelterin components. TRF1 and TRF2 are shown binding double stranded telomere sequence. POT1 binds single stranded telomere sequence. RAP1 associates with TRF2, TIN2 binds TRF1 and TPP1, which in turn bind POT1. C) Other telomere related proteins RTEL1, PARN, and TCAB1.

telomeric sequence and allows telomerase to add new nucleotides to the end of chromosomes by reverse transcription (Armanios and Blackburn, 2012; Schmidt and Cech, 2015). Telomerase is only active in select cells within our body such as stem cells that need to maintain high proliferative potential and thus keep regenerative capacity after many rounds of cell division.

Mutations that prevent telomerase from elongating telomeres can cause a spectrum of diseases called the telomere syndromes. Although the clinical manifestations of the disorders vary, they are all caused by shortened telomeres (Armanios, 2009; Armanios and Blackburn, 2012). The most common presentation of the telomere syndromes is pulmonary fibrosis (Alder et al., 2008; Armanios and Blackburn, 2012; Armanios et al., 2007). Pulmonary fibrosis was first linked to telomeres when mutations in telomerase (TERT and TR) were found in families with pulmonary fibrosis (Armanios et al., 2007). Since that time mutations in DCK1, RTEL1, PARN,

TIN2, NOP10, NHP2, and NAF1 have all been found in patients with pulmonary fibrosis (Alder et al., 2015; Martinez and Blasco, 2017; Stanley et al., 2016; Stuart et al., 2015) (Table 1).

Familial pulmonary fibrosis is a genetic disorder that displays autosomal dominant inheritance (Borie et al., 2015; Planas et al., 2017). Mutations in telomerase components or other telomere related proteins currently account for 25% of familial pulmonary fibrosis cases (Alder et al., 2011; Alder et al., 2015; Fingerlin et al., 2013; Hoffman et al., 2016; Kropski et al., 2016). Sporadic pulmonary fibrosis cases also occur in which there is no family history of pulmonary fibrosis. It was recently discovered that 11% of patients with sporadic pulmonary fibrosis also have mutations in telomere related genes (Petrovski et al., 2017). Additionally, 25% of patients with sporadic pulmonary fibrosis and 37% of patients with familial pulmonary fibrosis have telomere lengths below the 10th percentile including patients without known telomere related mutations (Alder et al., 2008; Cronkhite et al., 2008). Short telomeres have also been associated with a poorer prognosis and decreased survival rate following lung transplant in pulmonary fibrosis patients (Dai et al., 2015; Newton et al., 2017).

Additionally, telomere syndromes including pulmonary fibrosis display genetic anticipation, which means that each subsequent generation becomes symptomatic at an earlier age (Armanios and Blackburn, 2012; Armanios et al., 2005). This is caused by mutations in telomere related genes that prevent length maintenance of the telomeres in gametes resulting in parents passing on shorter telomeres to their offspring (Armanios, 2012; Barbaro et al., 2016). The shorter inherited telomere length causes disease symptoms earlier in each generation. Together these findings highlight the important role of telomere length in the pathology of pulmonary fibrosis.

Table 1: Telomere Genes Known to Cause Pulmonary Fibrosis When Mutated

Telomere Genes Known to Cause Pulmonary Fibrosis When Mutated	
Process/Complex	Gene
Telomerase Core Components	TERC TERT
Telomerase Biogenesis	DKC1 NOP10 NHP2
Sheltrin Component	TIN2
Telomeric DNA Synthesis	RTEL1
TERC RNA Processing	PARN NAF1

Despite these findings, the genetic basis for the majority of familial pulmonary fibrosis cases is still unknown. One potential area for the discovery of more genes is in the telomere length maintenance pathway. The mechanism of adding new telomere sequence is not yet fully understood and there may be key components of the pathway that are still unknown. Finding new genes involved with this process will allow for better diagnosis of telomere syndromes as well as further research into causes and cures.

Discovering new genes and the role that those genes play *in vivo* has recently been made more feasible through the use of the RNA-guided nuclease CRISPR associated protein 9 (Cas9)(Cong et al., 2013; Jinek et al., 2012). The clustered regularly interspaced short palindromic repeats (CRISPR)-Cas system was isolated from bacteria, where it plays an important role in adaptive immunity (Bhaya et al., 2011; Makarova et al., 2015). Cas9 is a site-

specific endonuclease that uses a guide RNA (gRNA) complimentary to the cut site in the genomic DNA (Bhaya et al., 2011). The double stranded break created by Cas9 can be repaired by non-homologous end joining (NHEJ) or homology directed repair (HDR) as seen in figure 2 (Chapman et al., 2012; Ran et al., 2013). NHEJ often results in small insertions or deletions that can disrupt the coding sequence of the gene and knockout protein function (Chang et al., 2017). Homology directed repair uses a DNA template to repair the cut site and is less error prone than NHEJ (Bibikova et al., 2001; Jasin and Rothstein, 2013).

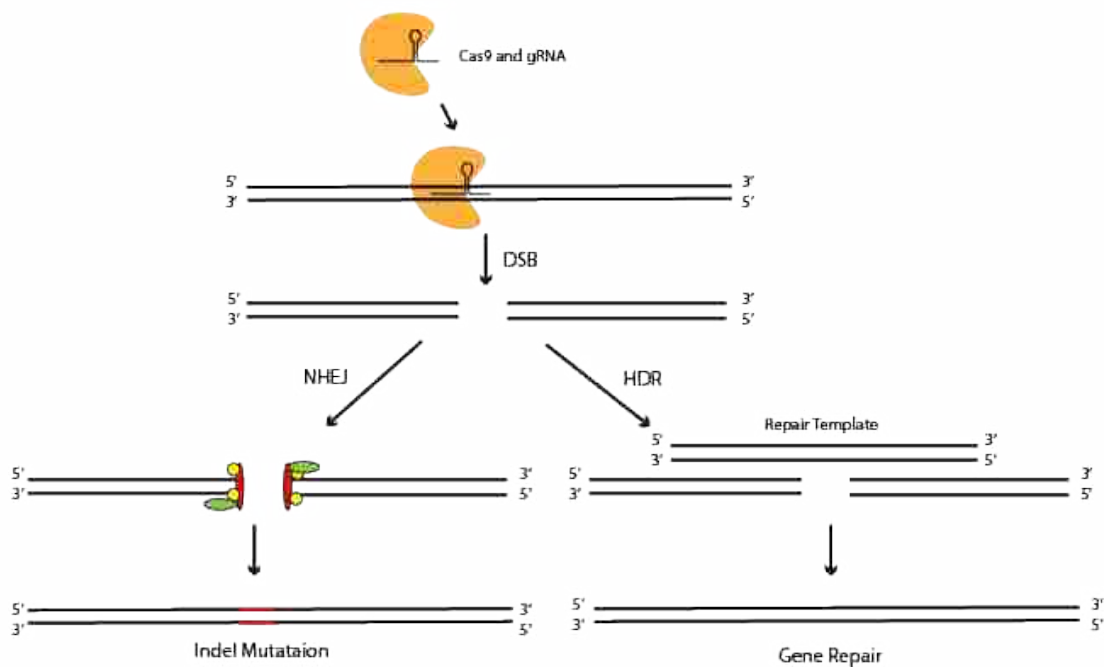


Figure 2: Cas9 Cutting and Repair. Cas9 associates with a gRNA which directs Cas9 to bind at a specific place in the genome. Cas9 then creates a double stranded cut in the DNA which can be repaired by the cell in one of two ways. 1) Non-homologous end joining (NHEJ)- The cell repairs the break by annealing the broken ends back together, which often results in small insertions or deletions called “indels”. These indels may result in non-functional proteins leading to gene knock out. 2) Homology Directed Repair (HDR)- The cell can use a template with homology to repair the break. This results in precise genome editing.

Both repair pathways can be utilized to study genes of interest. NHEJ can be used to knockout genes and HDR can be used to introduce new DNA sequence into a cut site (Sander and Joung, 2014). Addition of exogenous DNA is done by creating templates that include homology around the Cas9 cut site and the new DNA sequence you want to introduce (Mali et al., 2013).

Using Cas9 for genome editing has made studying the function of proteins much more effective. There are multiple techniques available for introducing CRISPR-Cas9 into cells including transduction, nucleofection, and transfection (Bisht et al., 2017; Dow et al., 2015; Kim et al., 2014). Nucleofection has been shown to be effective in introducing Cas9 and its components into cells, however, it requires specialized equipment and materials that can be expensive and may not be available to every lab. Transduction also has limitations as the use of virus requires extra biosafety precautions, which may not be ideal. That means that not all labs may be able to utilize the CRISPR-Cas9 system. Because of the usefulness of CRISPR-Cas9, there is a need to optimize its use to make it easily accessible in terms of time, money, and materials.

MATERIALS AND METHODS

Plasmid Construction

pSpCas9(BB)-2A-Puro (PX459) V2.0, a gift from Feng Zhang (Addgene #62988), was used to construct Cas9 and gRNA expressing vectors according to previous published protocols (Ran et al., 2013). pCDNA5/FRT-EGFP and Δ ATG-EGFP plasmids were constructed using Gibson Assemblies following standard procedures. A puromycin-expression plasmid was generated by cloning the puromycin N-acetyl-transferase gene in an SV40-expression cassette into the pBluescript II KS(+) vector. The lentiCas9-blast plasmid, a gift from Feng Zhang (Addgene #52962), was used to stably express Cas9 in cell lines according to previous published protocols (Sanjana et al., 2014). The hTR-WT and MT-hTR-AU5 GFP expressing plasmids were a kind gift from Bradley Stohrs (Stohr et al., 2010). Lentiviral plasmids carrying puromycin resistance and coding for gRNAs designed to target *TERT* and *ZNF827* were created by cloning a gRNA to *TERT* and *ZNF827* respectively into lentiGuide-Puro, a gift from Feng Zhang (Addgene #52963). Human Brunello CRISPR knockout pooled library was a gift from David Root and John Doench (Addgene #73178) (Doench et al., 2016b).

Cell Culture and Transfection

HeLa cells were purchased from the ATCC (Cat #CCL-2). HEK 293 FlpIn cells were purchased from Invitrogen and both cell lines were cultured in Dulbecco's Modified Eagle's medium (DMEM, Gibco) supplemented with 10% fetal bovine serum (FBS, Gibco), 0.29 mg/ml L-Glutamine, 100 U/ml penicillin, and 100 μ g/ml streptomycin (Gibco). Cells were grown in a 37°C humid incubator with 5% CO₂. HEK 293 FlpIn Cells were transfected with the EGFP or Δ ATG-EGFP plasmids described above according to manufacturer's protocols and selected with hygromycin. Cas9 stable cell lines were generated by infecting cells with a Cas9-expressing

lentivirus (Addgene plasmid #52962). All px459v2, RNP, and RNA only transfections were done in 24 well plates using 1 ul of Lipofectamine 2000 (Invitrogen) as the transfection reagent. Plasmid transfections were done using 0.5 µg of plasmid. RNP transfections used 250 ng pBS Pur, 100 ng gRNA and 0.5 µg of cas9 purified protein. In RNP transfection Cas9 and the gRNA were incubated at room temperature for 5 minutes prior to the addition of pBS Pur. In RNA only transfections 250 ng pBS Pur and 100 ng of gRNA were used. Donor template concentration was optimized for each transfection type. 500ng of template was used in plasmid transfection, 50 ng of template was used in RNP transfections, and 10 ng of template in RNA only transfections. 24 hours after transfection 2µg/ml of puromycin was added to the cells. The cells were incubated in puromycin for 48 hours after which the selection reagent was removed from the cells. Individual clones of cells were isolated by limiting dilution. LOX melanoma cells were a kind gift from Bradley Stohrs and were cultured in Roswell Park Memorial Institute (RPMI, Gibco) supplemented with 10% fetal bovine serum (FBS, Gibco), 0.29 mg/ml L-Glutamine, 100 U/ml penicillin, and 100 µg/ml streptomycin (Gibco).

Flow Cytometry and Microscopy

Cells were trypsinized and then neutralized using DMEM/10% FBS for HEK 293 cells or RPMI/10% FBS for LOX cells. The cells were mixed and the percentage of cells expressing EGFP was assessed using a BD Accuri Flow cytometer. Viable cells were gated using morphology and EGFP percentages of the viable cells were measured. Imaging of fluorescent proteins was performed on an Olympus IX70 microscope equipped with a MicroFire Color camera (Olympus) using a 20x objective. Cell sorting of LOX cells was performed using a FACS Aria Fusion. Cells were first trypsinized, rinsed, and suspended in PBS/2% FBS. The cells were sorted for GFP and collected in RPMI/10% FBS cell culture media.

Genomic DNA Collection, Screening, and Sequencing of Modified Clones

Genomic DNA was isolated from individual clones by suspending cells in lysis buffer (300 μ l; 10mM Tris-HCL, 25mM EDTA, 0.5% SDS, pH 8), precipitating protein by addition of salt (100 μ l; 5M Ammonium Acetate), and extraction of DNA with ethanol. PCR was performed using primers flanking the Cas9 cut site and amplicons were cloned using zero-blunt cloning (Invitrogen). Several colonies from each cloned amplicon were Sanger sequenced to characterize individual mutations.

Donor Template Creation

Single stranded donors for ATG and ATG-FLAG were synthesized by IDT with 30 base pairs of homology on the 5` and 3` ends. Double stranded templates for ATG-RFP knock-in was generated by PCR amplification and incorporated a short linker on the C-terminus of RFP and 35 base pairs of homology on either end.

Western Blots

Western blots were carried out using standard procedures. Briefly, 20-40ug of cell lysate was separated on a 4-12% SDS-PAGE gel and transferred to nitrocellulose membranes. Membranes were blotted with Flag (M2; Sigma), GFP (Aves Laboratories), KEAP1 (Cell Signaling Technologies), GAPDH (Santa Cruz Biotechnology), and secondary antibodies (Licor) and imaged on an infrared scanner (Licor).

Protein Purification

Cas9 was expressed in BL21(DE3) cells using pET-28b-Cas9-His, a gift from Alex Schier (Addgene plasmid # 47327)(Gagnon et al., 2014). Following overnight induction with IPTG at 18C, bacterial were harvested and lysed in lysis buffer (20mM Tris pH8, 500mM NaCl,

and protease inhibitors [Sigma]). Bacteria were lysed using sonication or high-pressure microfluidic shearing and the lysate was centrifuged at 15,000g for 20 minutes. Clarified supernatants were mixed with 2mL of Nickle Beads (BioRad) and mixed for 1 hour at 4C. The suspension was poured into a gravity column and washed with wash buffer (20mM Tris pH8, 50mM NaCl, 25mM imidazole). Cas9 was eluted (20mM Tris pH 8, 500mM NaCl, 250mM Imidazole) and dialyzed into storage buffer (20mM Tris pH 8, 500mM KCL, 10mM MgCl₂, 50% glycerol).

In Vitro Transcription and *In Vitro* Cutting with Cas9

Primers were constructed containing a T7 transcription site as well as a guide RNA sequence (see supplemental table of primers). We used the plasmid pSpCas9(BB)-2A-Puro as a template for PCR to create a product with a T7 transcriptional start site, gRNA sequence, and gRNA scaffold. In vitro transcription was performed with a MEGAshortscript T7 Transcription kit (Invitrogen) per the manufacturer's protocol. RNA was isolated using a phenol chloroform extraction and diluted in water to 1µg/µl. The RNA was then stored in aliquots at -80°C. To test the functionality of the RNP we performed an in vitro digestion with 200 ng target DNA, 100 ng gRNA, 1µl BSA (NEB), 1µl NEB buffer 3, 1 µg Cas9, and water assembled into a 10 µl reaction. This mixture was incubated at 37°C for 1 hour followed by a 10-minute incubation at 65°C. Digestion products were separated on a .75% agarose gel.

Hydrogen Peroxide Challenge

KEAP1-targeted and parental HeLa cells were cultured in a 96-well plate and exposed to increasing concentrations of H₂O₂ (0-250 µM) for 24 hours. Following exposure, cell viability

was measured using an 3-[4,5-dimethylthiazol-2-yl]-2,5 diphenyltetrazolium bromide (MTT) using previously described methods(van de Loosdrecht et al., 1994).

Viral Packaging and Transduction

Viruses were packaged in 293 FT cells in DMEM (Gibco) containing 1% FBS (Gibco). Transfections were done using a 4:3:1 ratio of viral plasmid, to psPax2, to pMD2.G following the lipofectamine 2000 protocol. Virus was collected 48 and 72 hours post transfection and concentrated using centrifugal filters. Transduction was done using 8ug/ml polybrene and the packaged virus. The media was changed the following day.

Telomerase Repeated Amplification Protocol (TRAP) Assay

TRAP assay was performed according to previously published protocol (Mender and Shay, 2015). Briefly, 100,000 cells were collected and suspended in NP-40 solution on ice for 30 minutes. A TRAP master mix was prepared and 1ul of sample was added to each tube. Cy5 primers were used so results could be visualized by fluorescence. Amplification of the extension products was then performed by PCR according to the published protocol. The samples were run on a 10% non-denaturing polyacrylamide gel at 250 V. The results were visualized on a licor imaging system.

Forward Genetic Screen

Human Brunello CRISPR knockout pooled library was a gift from David Root and John Doench (Addgene #73178) (Doench et al., 2016b). LOX melanoma Cas9 Blast cells were first transduced with Human Brunello CRISPR knockout pooled library (Human GPP library) at an MOI of 3. After 48 hours the cells underwent puromycin selection. Following puromycin selection MT-hTR-AU5 was added at an MOI of 10. After 15 days the cells were sorted for GFP

positive cells. The cells were then allowed to grow for two weeks before being sorted again and collected for genomic DNA.

GeCKO PCR and Deep Sequencing

The gRNAs were amplified using a two-step PCR procedure. The first PCR was done in 4 reactions each with 5 ug of pooled genomic DNA. The thermocycling parameters for the PCR 95°C for 2 min and 18 cycles of 95°C for 20s, 65°C for 30s, and 72°C for 30s followed by 72°C for 5 min. The second PCR added the barcodes for Illumina sequencing. The PCR products from the first PCR were pooled and 5 ul of that was added to the second PCR. The thermocycling parameters for the PCR 95°C for 2 min and 25 cycles of 95°C for 20s, 61°C for 30s, and 72°C for 30s followed by 72°C for 5 min. The concentration of DNA in each barcode was quantified using the Next Library Quantification kit (New England Biolabs, Inc.). After quantification each sample was diluted to 10nM and mixed in equal amounts with all other samples. The pooled samples were again quantified and then diluted to 2.5nM. The diluted libraries were then sequenced with MiSeq instrument (Illumina).

Data Analysis

We used GraphPad Prism v7 for analysis and generation of graphs. Means were compared using Student's t-test. P values ≤ 0.05 were considered significant and all values shown are two-sided. Data analysis of the deep sequencing data was evaluated using custom perl script. Bowtie was used to align the gRNAs to genes and MaGeCK was used to rank genes. Significance for the ZNF827 verification experiment was calculated using ANOVA followed by a TukeyHSD analysis in R.

RESULTS

CRISPR-Cas9 Optimization

RNP Lipofection Showed Highest Efficiency of Knockout

In order to make CRISPR-Cas9 more accessible, we decided to determine the most effective method for gene knockout using cationic lipid-mediated transfection (lipofection) to introduce Cas9 components into cells. For transfections we used an HEK 293 FlpIn cell line in which a single copy of EGFP had been inserted into the FRT site using Flp recombinase. This cell line allowed for easy quantification of the effectiveness of GFP knockout using flow cytometry. We also created an HEK 293 FlpIn EGFP Cas9 clonal cell line to test RNA only transfection into stably expressing Cas9 cells (Figure 3A). We decided to compare the knockout efficiency of transfection of a plasmid encoding Cas9 and gRNA, a Ribonucleoprotein (RNP) containing Cas9 and gRNA, and gRNA only into a Cas9 expressing cell line. For the plasmid and RNP transfections we used the HEK 293 FlpIn EGFP line and for the RNA only transfection we used the HEK 293 FlpIn EGFP Cas9 blast cell line.

For the RNP and RNA only transfections a gRNA was created through a reverse transcriptase reaction. In order to test that the synthesized gRNA was functional, an *in vitro* Cas9 cutting experiment was performed (Figure 3 B). A template for cutting was created through PCR using an EGFP plasmid. The template, gRNA, and Cas9 were incubated and then run on a agarose gel. The template was cut in the presence of Cas9 and the gRNA indicating that the gRNA successfully directed Cas9 cutting (Figure 3B).

In order to determine the most effective transfection reagent, we compared lipofectamine 2000, lipofectamine CRISPRmax, and lipofectamine RNAimax, and found lipofectamine 2000 transfection to be the most effective and least harmful to the cells (optimization not shown). We

continued our experiments using lipofectamine 2000 to compare plasmid, RNP, and RNA only transfections. After transfection, cells were allowed to grow for 5 days before GFP percentage was measured through flow cytometry. Plasmid, RNP, and RNA only transfections all showed some level of GFP knockout, however, without selection the levels of GFP knockout were low (Figure 3D).

In order to increase the effectiveness of GFP knockout, we decided to co-transfect a selection plasmid that would confer resistance to puromycin. The plasmid px459v2 already carries resistance to puromycin, so for the RNP and RNA only transfections we co-transfected a plasmid expressing puromycin N-acetyl-transferase (PAC) which confers resistance to puromycin. One day after transfection, puromycin was added and the cells were left in selection for 48 hours. The cells were passaged until 5 days after transfection when the cells were collected for flow cytometry to measure GFP percentage. Representative flow data of a successful RNP transfection is shown in Figure 3C. The percentage of GFP negative cells were quantified for each condition and the results are shown in Figure 3D.

All conditions showed some level of GFP knockout which was increased with the addition of a selection reagent showing that at least one limiting factor in successful gene editing is transfection efficiency. Of the methods tested, RNP transfection with puromycin selection was the most effective.

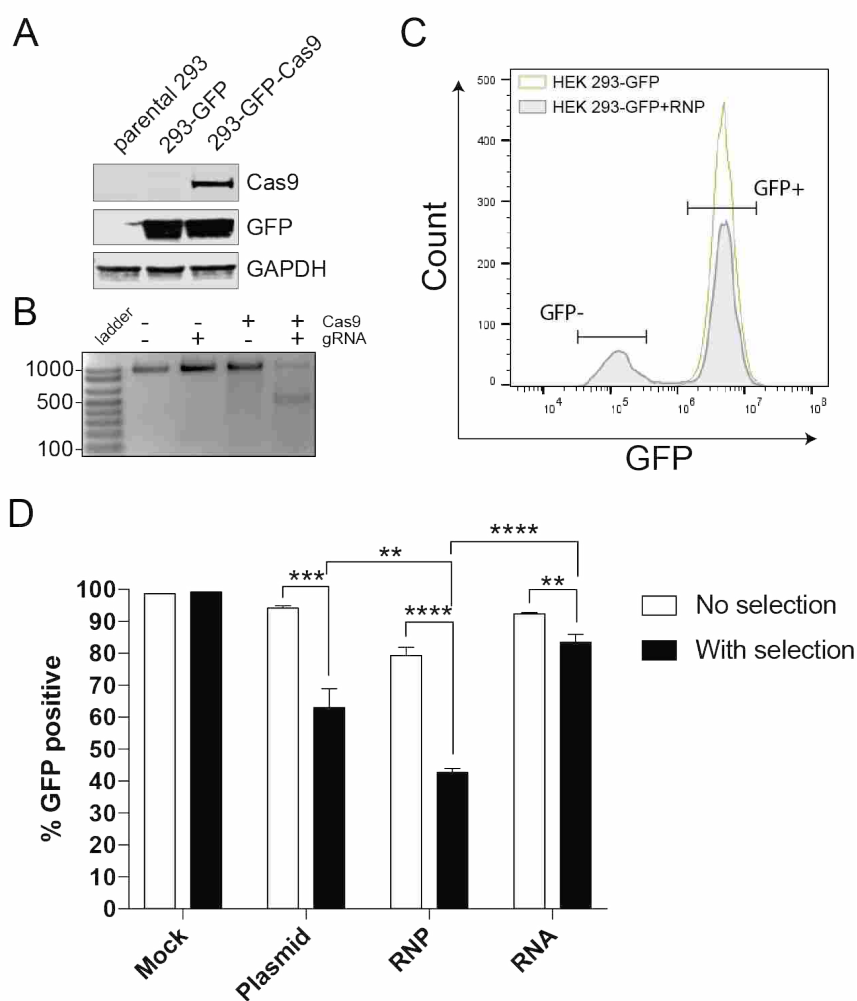


Figure 3. Comparison of Methods to Introduce Cas9 and Guide RNAs. A) Western Blot of HEK 293 FlpIn Lines Expressing GFP Reporter and Cas9. GFP was introduced at FlpIn locus to ensure that only a single copy of the target gene was present; Cas9 was introduced by infecting cells with a lentivirus encoding flag-tagged Cas9 (see materials and methods). B) *In Vitro* Digestion of Target DNA by RNP Complex. A 1000 base pair (bp) amplicon was generated by PCR amplification of a GFP-containing plasmid. Digestion of the amplicon results in two 500 bp segments. C) Representative Histogram of Flow Cytometry Data Demonstrating Disruption of GFP by Cas9. The histogram shows viable cells five days post transfection with a GFP-specific RNP. The green line represents control cells (GFP+) and the grey line represents GFP+ cells that had been transfected with a GFP-specific RNP. D) Quantification of the Fraction of GFP Positive Cells Remaining After Treatment with Cas9 and gRNA Using Different Methods of Introduction (n=3/group). Data are expressed as mean \pm SEM. ** $P < 0.02$, *** $P < 0.001$, and **** $P < 0.0001$; Student's *t*-test.

Knocking Out Endogenous Genes Using RNP Transfection

Using the conditions found to be the most effective at knocking out GFP in the HEK 293 FlpIn EGFP reporter system, we attempted to knockout endogenous genes. We designed 1-2 gRNAs targeted at the 5' coding region for both telomerase reverse transcriptase (*TERT*) and kelch like ECH associated protein 1 (*KEAP1*) using the Broad GPP portal design tool (<http://portals.broadinstitute.org/gpp/public/>). Before transfection we tested the gRNAs through a Cas9 *in vitro* digest using PCR amplified regions of the genes as templates for cutting (Figure 4A and 4B). After successful *in vitro* cutting, we moved to lipofection into cell lines. We decided to use two common cell lines, HEK 293 and HeLa, to make our experiments widely applicable.

We performed RNP transfection with gRNA targeted at *TERT* into HEK 293 cells, selected with puromycin, and isolated clones. Genomic DNA was collected from the clones and PCR was performed around the Cas9 cut site in each clone to see if there were obvious band shifts or mutations in any of the clonal cell populations. As can be seen in Figure 4C some of the clones had obvious mutations in the cut site region of *TERT*. To ensure that these cells had deleterious mutations in all of the alleles of *TERT* we subcloned to sequence each allele. An example of sequencing from a knockout clone is shown in Figure 4D. We found a 1bp frameshifting insertion in one allele and a 250bp insertion in the other allele confirming that this cell population should have no functional TERT.

Interestingly our attempts to disrupt KEAP1 through RNP transfection in HeLa cells were unsuccessful after numerous attempts despite the gRNA showing functionality in the Cas9 *in vitro* digestion (Figure 4B). We therefore turned to plasmid transfection for the knockout of KEAP1 using px459v2 designed to target *KEAP1*. After plasmid transfection, clones were readily isolated and genomic DNA was collected. PCR of the clones was performed around the

Cas9 cut site and many bands were seen indicating mutations in *KEAP1* (Figure 4E). We again subcloned cell populations that looked as if they had multiple mutations and sequenced individual alleles. Figure 4G shows the sequencing of one of these clones which had a 1bp insertion in one allele and a 1bp deletion in the other copy of *KEAP1*. The knockout of KEAP1 was further confirmed through western blot (Figure 4F). Additionally, we wanted to verify that knockout of KEAP1 was showing the expected physiological effect. KEAP1 is a negative regulator of Nuclear factor (erythroid-derived 2)-like 2 (NRF2). Nrf2 is a transcription factor that binds to the anti-oxidant response element (ARE) and turns on transcription of antioxidant proteins (Hayes and McMahon, 2001; Katoh et al., 2005; Sihvola and Levonen, 2017). When KEAP1 is knocked out we should see an upregulation of Nrf2 activity, which protects the cell from cytotoxic effects of oxidants. To test this, we dosed the cells with varying degrees of H₂O₂ and measured the percent of cells that survived. Cells with KEAP1 knocked out showed a much higher resistance to H₂O₂ confirming that the knockout of KEAP1 was having the expected physiological effect (Figure 4G).

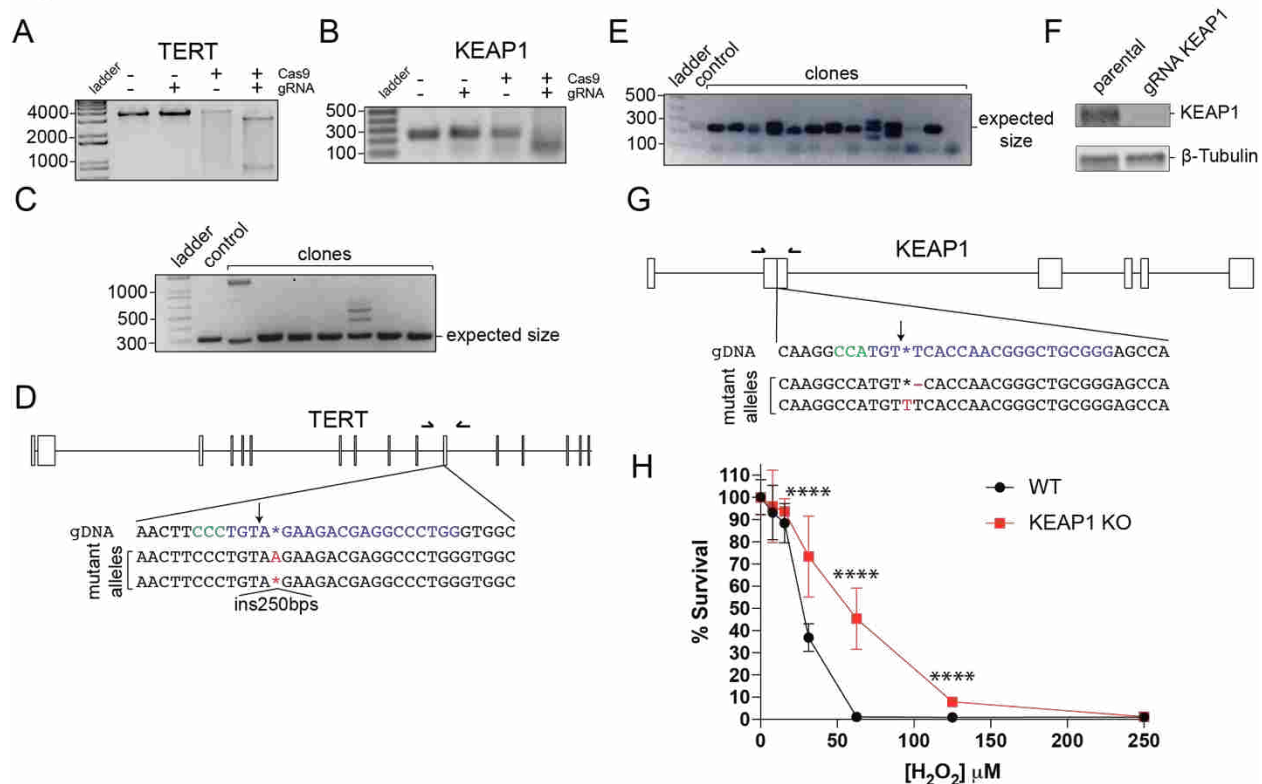


Figure 4. RNP Mediated Disruption of Endogenous Genes. A) *In vitro* digestion of DNA Fragment Containing Sequence Complementary to TERT gRNA Sequence. A target substrate was generated by digestions of a plasmid containing TERT cDNA to yield a 3.6 kb product. Digestion of the product with RNP yields a 2.8 kb and 800 bp band. B) *In Vitro* Digestion of Amplicon Containing KEAP1 cDNA Sequence. A substrate was generated by PCR amplification of a 250 bp fragment containing the KEAP1-targetting sequence. Digestion with KEAP1-specific RNP yields a 150 and 100 bp products. C) PCR of Genomic DNA from *TERT*-Targetted Clones Showing Amplicon Size Heterogeneity in Several Clones. Approximate primer positions shown in D. D) Schematic and Sequencing Results from One Clone Showing Frame Shifting Mutations in 2 Out of 2 Alleles Detected. PCR products from C were sub-cloned using zero-blunt cloning, so that individual alleles could be sequenced. 16-18 subclones were sequenced for each independent clone. The number of alleles is inferred from the number of unique sequences that were detected. E) PCR of Genomic DNA from *KEAP1*-targetted Clones Showing Amplicon Size Heterogeneity in Several Clones. Approximate primer positions shown in G. F) Western blot for showing loss of protein in targeted cells. G) Schematic of *KEAP1* Gene and Location of gRNA. Protospacer adjacent motif (PAM) sequence (green) and Cas9 cut site (arrow) are depicted. Note, the gRNA target sequence was located on the opposite strand of DNA. Frameshifting mutant alleles are shown from sequencing sub-cloned PCR products. H) *KEAP1*-deficient Cells were Functionally Tested by Challenging with an Oxidant (H_2O_2). Cell viability was measured using MTT assay 24 hours post exposure to increasing concentrations of H_2O_2 . Error bars show SEM for each measurement. Data are expressed as mean \pm SEM. **** $P < 0.0001$; Student's *t*-test.

Comparison of Methods for Cas9-mediated Genome Editing Using a Reporter System

Genome editing using CRISPR-Cas9 is an exciting field that utilizes the cells natural homology directed repair response to incorporate exogenous pieces of DNA into the genome (Ran et al., 2013). However, genome editing in the past has been reported at very low rates meaning that researchers had to screen many clones to find a successfully edited population (Bialk et al., 2015; Bialk et al., 2016). We wanted to improve not only the efficiency of genome editing, but also the accessibility, by optimizing CRISPR-Cas9 genome editing using lipid-mediated transfection.

To best quantify the effectiveness of editing, we again used the HEK 293 FlpIn cell line, but inserted an EGFP lacking the ATG start codon into the FRT site. This cell line is GFP negative, but becomes GFP positive with the successful insertion of an ATG at the genome editing site (Figure 5A). We also created an HEK 293 FlpIn Δ ATG EGFP Cas9 cell line that stably expresses Cas9 protein. Using these two cells lines we compared knock-in efficiency using plasmid to express Cas9 and gRNA, RNP, and gRNA only into stably expressing Cas9 cells. In all of these transfections a single stranded oligonucleotide containing the ATG to be inserted and 30bp homology arms was also included (Figure 5B). To verify the effectiveness of the transcribed gRNA, an *in vitro* Cas9 digestion was performed prior to transfection. A PCR amplified region of a plasmid containing Δ ATG EGFP was used as a template and incubated with Cas9 and a gRNA directed to cut Δ ATG EGFP 5 bp from the ATG insertion site. The *in vitro* digestion showed successful cutting, so we decided to move forward with knock-in transfections (Figure 5B).

To confirm that our reporter system worked and to determine how long it took for GFP to accumulate to detectable levels, we first tried all transfections without any selection reagent and

examined the cells for fluorescence. We were able to see a few GFP positive cells after only 24 hours indicating that the knock-in was successful. We determined that waiting 5 days post transfection allowed the cells enough time to accumulate GFP to maximize fluorescence. The first rounds of transfection without selection did have successful knock-in, but at a low efficiency as we expected due to the results of our knock out experiments. Since our goal was to optimize efficiency of knock-in, we decided that co-transfection of a selectable marker would be key to increasing the knock-in percentage.

We next tried transfection followed by puromycin selection. The px459v2 plasmid used already confers puromycin resistance, so for the RNP and RNA only transfections we again co-transfected a plasmid expressing puromycin N-acetyl-transferase (PAC). 24 hours after transfection, puromycin was added for 48 hours. Flow cytometry was performed 5 days post transfection to measure GFP percentage. A representative of the GFP flow data is shown in Figure 5C. A GFP population is present after RNP transfection that was not present in the HEK 293 FlpIn Δ ATG EGFP population before transfection (Figure 5C). Puromycin selection greatly increased the percentage of cells that were successfully edited, showing again that transfection efficiency is a limiting factor in lipofection mediated Cas9 editing.

We next sought to optimize the amount of donor template that should be transfected along with plasmid, RNP, or RNA only transfections. Papers have cited varying optimal concentrations of donor template, so we wanted to determine the ideal concentration for Cas9 editing using lipofection (Lin et al., 2014; Moyer and Holland, 2015). We tried 500 ng, 100ng, 50 ng, and 10 ng of donor template with each of the three methods of Cas9 introduction. Interestingly the amount of template that produced the best results varied by Cas9 expression type. Plasmid transfections were best with 500 ng of template, whereas RNP transfections were

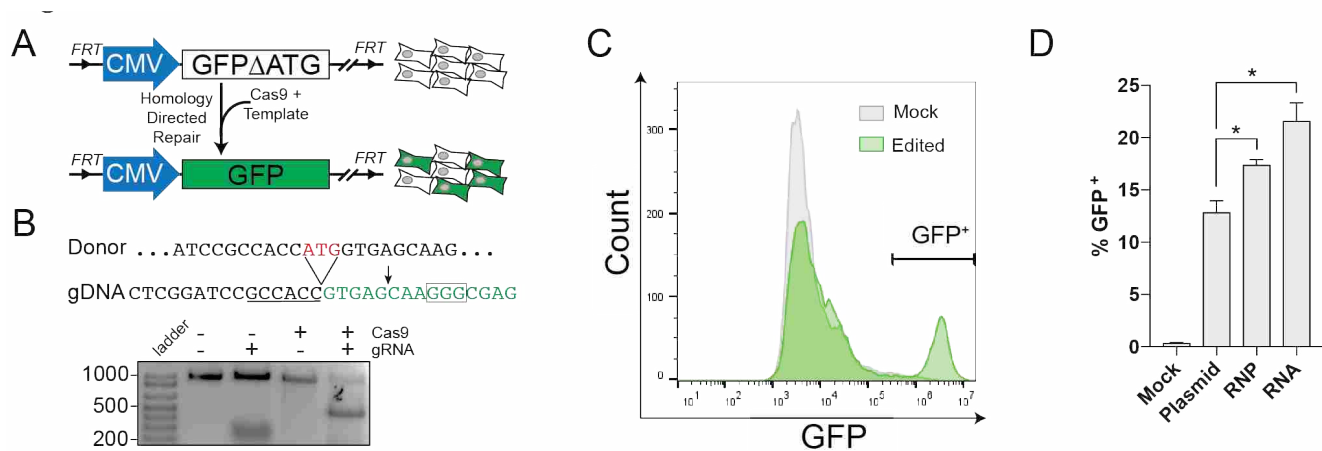


Figure 5. Comparison of Methods for Inserting Exogenous Sequences. A) A Reporter System for Detection of HDR-mediated Introduction of Exogenous Sequences. A single Δ ATG-EGFP cassette was inserted at the Fln locus in HEK 293 cells. Introducing an ATG at the 5' end of the cassette results in GFP positive cells. B) Schematic of Target and Donor DNA and *In vitro* Digestion with RNP. The exogenous ATG (red) is shown in the donor. Kozak sequence (underlined), Cas9 cut site (arrow) and PAM (box) is shown in the target gDNA. *In vitro* digestion was done using a 1000 bp PCR product of Δ ATG-EGFP. Digestion with RNP results in two 500bp segments. C) Representative Histogram of Control and Edited Cells Showing the Shift in GFP Fluorescence Five Days Post Transfection. D) Quantification of the Fraction of GFP Positive Cells After Treatment with Cas9, gRNA, and Donor DNA Using Different Methods of Introduction (n=3/group). Data are expressed as mean \pm SEM. * $P < 0.05$; Student's *t*-test.

most effective with 50 ng of template, and RNA only transfections produced the best results with 10 ng of template (Data not shown). This variation in concentration may be due to the different methods of Cas9 expression.

The best concentration for each of the transfection methods is compared in Figure 5D. Transfection of gRNA only into Cas9 expressing cells had the overall highest editing rate, however, very few cells survived selection in this method. We had to let the cells grow out for 7 days in order to get enough cells to measure through flow cytometry and only the transfections containing small amounts of donor template had any living cells. This means that although there

are a high percentage of edited cells in RNA only transfections, it may not be the most effective method due to the few number of cells surviving selection. Again RNP showed a high level of editing and more cells were able to survive selection making this a more reasonable approach for knock-ins.

Larger Knock-ins Using a Reporter System

One benefit of the reporter system we created is the ability to knock-in a variety of tags to the genome editing site. This is a distinct advantage over previous GFP reporter systems that only express GFP with the correction of one base pair (Bialk et al., 2016; Richardson et al., 2016; Rivera-Torres et al., 2017). We decided to attempt to knock-in two commonly used tags, FLAG and RFP at the Δ ATG site (Figure 6A). With knock-in of either tag the cells also express GFP allowing for easy quantification of knock-in percentage.

The ATG and FLAG donor templates were single stranded oligonucleotides with 30bp homology arms. The RFP template was created through PCR and was therefore double stranded. We ordered primers to amplify RFP that also contained 35bp of homology to the knock-in site in Δ ATG. Amplifying RFP through PCR to create a donor template was quick, effective, and inexpensive. This technique greatly simplifies the insertion of large pieces of DNA since the cloning of donor templates with long homology arms can take days or weeks.

For all experiments we used RNP transfections using the ideal conditions found in our previous optimization. All knock-in experiments were successful, however, as the size of the insert went up, the efficiency of knock-in decreased (Figure 6B). We also did a western blot for GFP to confirm the expression of GFP (Figure 6C). Interestingly we found that some cells expressed GFP with RNP transfection alone. We confirmed that an 8bp deletion would result in an in frame ATG start codon. Images of cells edited with RFP donor template also show that all

RFP positive cells are also GFP positive, however, there are a number of GFP positive cells without RFP expression. Overall we found that knock-in of larger templates is possible, however, the efficiency may go down as the size of the insert increases.

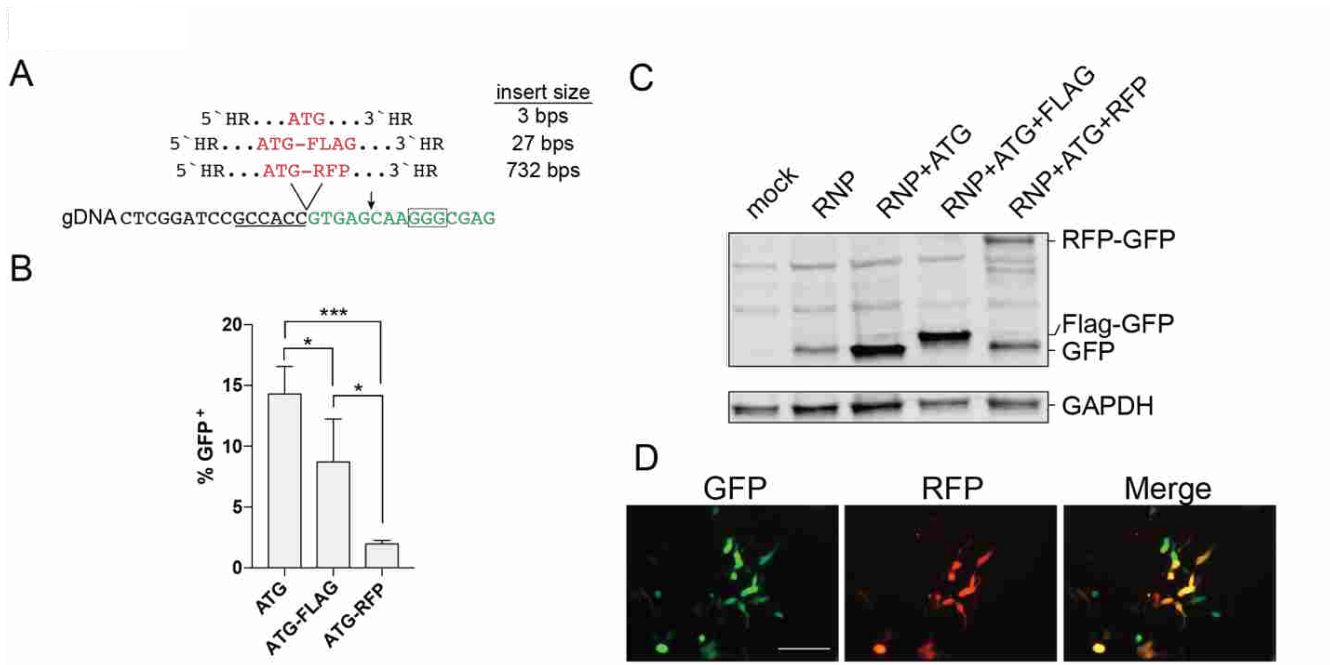


Figure 6. Introduction of Epitope Tags and Fluorescent-protein Tags Using RNP Transfection. A) Schematic of Donor Templates that were Inserted into our Reporter Construct. Size of the inserted DNA is shown on the right. Kozak sequence (underlined), Cas9 cut site (arrow) and protospacer adjacent motif (PAM; box) is shown in the target gDNA. B) Fraction of GFP Positive Cells After RNP Transfection with Different Donors (n=3/group). C) Western blot with Anti-GFP Antibody Showing GFP and Modified-GFP After Editing. D) Representative Immunofluorescence Images of Edited Cells Showing Co-localization of GFP and RFP Fluorescence. Scale bar is 100 μ m. Data are expressed as mean \pm SEM. * $P < 0.05$; Student's t -test.

Forward Genetic Screen for Telomere Length Maintenance Genes

Knockout of TERT Protects Cells from MT-hTR-AU5 Transduction

In order to design a forward genetic screen in which we could identify new genes involved in telomere length maintenance, we first needed to find a proper selection agent. Recent publications described MT-hTR-47A and MT-hTR-AU5 viruses which are predicted to add mutated telomere sequences to the end of chromosomes and have been shown to cause cell senescence and apoptosis (Stohr and Blackburn, 2008; Stohr et al., 2010). Shelterin recognizes and binds to wild type telomere sequence, so addition of mutated telomere sequence is predicted to disrupt telomere-shelterin binding and trigger a DNA damage response. Before attempting a forward genetic screen we tested if these viruses caused cellular senescence or apoptosis and if disrupting the telomere length maintenance pathway could rescue transduced cells.

We first sought to verify the toxicity of MT-hTR-47A and MT-hTR-AU5 in cell lines routinely used on our lab. Unexpectedly, HEK 293 and HeLa cells did not appear to be sensitive to the template mutants and grew readily even in the presence of high viral titers (data not shown). We found that the toxicity of these viruses varies by cell line and that the addition of mutated telomere templates was most detrimental to LOX melanoma cells (a telomerase positive human cancer cell line)(Goldkorn and Blackburn, 2006; Stohr and Blackburn, 2008). We compared MT-hTR-47A and MT-hTR-AU5 and found MT-hTR-AU5, which is predicted to add “TATATA” to the end of telomeres, to be more lethal to LOX cells and therefore decided to move forward using MT-hTR-AU5.

To show that disruption of the telomere length maintenance pathway could protect against MT-hTR-AU5 transduction, we tested the survival of LOX cells transduced MT-hTR-AU5 in which telomerase reverse transcriptase (TERT) had first been knocked out. After cloning

LOX Cas9 cells, we transduced a population of cells with a lentivirus encoding a gRNA directed to *TERT* and then selected with puromycin 48 hours after the addition of virus. We hypothesized that cells that were deficient for TERT would be resistant to MT-hTR-AU5 transduction since the knockout of TERT disrupts the addition of new telomere sequence. After multiple trials we found that it was important to use cells as quickly after selection for TERT knockout since cells lacking TERT have a growth disadvantage. MT-hTR-AU5 and hTR-WT, which codes for wild type telomere sequence, were added to LOX Cas9 cells and TERT knockout LOX Cas9 cells. Both MT-hTR-AU5 and hTR-WT viruses were packaged from a lentiviral plasmid that also expresses GFP, so all transduced cells also expressed GFP. In order to measure the number of living cells containing virus, the GFP percentage was measured through flow cytometry every 2-3 days post transduction. As can be seen in Figure 7A, the wild type virus had no effect on the transduced cells and the GFP percentage remained constant throughout the experiment. However, we saw varying results with MT-hTR-AU5 viral transduction. The LOX Cas9 cells containing the virus were nearly gone by two weeks post infection reproducing previously reported data (Stohr and Blackburn, 2008; Stohr et al., 2010). On the other hand, TERT knockout LOX cells had an initial drop in GFP percentage, but then the level of GFP stayed constant around 35-40% (Figure 7A).

We hypothesized that this initial drop in GFP percentage in the TERT knockout cells may have been due to incomplete knock out of TERT in a portion of the population. In order to confirm our prediction, we sorted the TERT knock out cells into GFP positive and GFP negative groups. We isolated 3 clones from each group and sequenced *TERT* in the GFP positive clones. These clones were significant because they were able to survive despite expressing MT-hTR-AU5. The sequencing of these clones showed frameshifting indels in all alleles, supporting our

theory that complete knock out of TERT protects cells from the MT-hTR-AU5 virus (Figure 7B). We also performed a Telomerase Repeat Amplification Protocol (TRAP) assay to show the activity of telomerase in these groups of cells. The three clones in the GFP positive group showed no telomerase activity, however, two of the three clones in the GFP negative group showed telomerase activity (Figure 7C). This confirmed our initial thought that transduction of the lentivirus containing a gRNA to *TERT* did not result in complete knock out of TERT in the entire population, which may explain the initial dip in GFP percentage in the TERT knockout group. Most importantly, we showed that cells that had a complete knockout of telomerase activity were able to survive transduction of MT-hTR-AU5. We concluded that MT-hTR-AU5 could be used in a forward genetic screen to identify genes involved in telomere length maintenance.

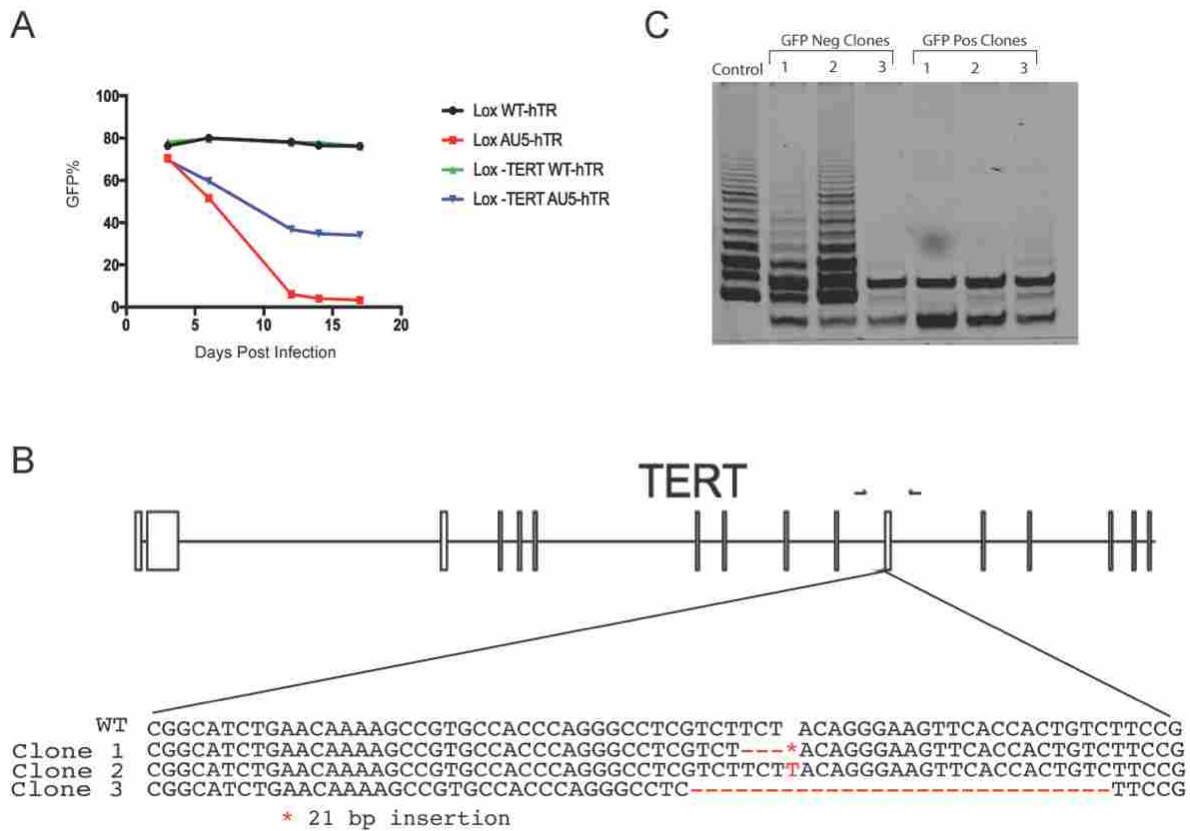


Figure 7: Knockout of TERT can Protect from MT-hTR-AU5 Infection. A) Transduction of WT-hTR Shows No Effect on LOX Cas9 and LOX Cas9 Ig-hTERT cells. LOX Cas9 cells transduced with AU5-hTR are almost completely dead 14 days after infection. LOX Cas9 cells that first had hTERT knocked out show some cell death initially, but remain 35-40% GFP positive after infection with AU5-hTR. B) Sequencing of Clones that Remained GFP Positive After MT-hTR-AU5 Transduction Show Detrimental Mutations to hTERT. One allele is shown from each of the clones sequenced as a representation of sequencing results. In each clone all alleles were mutated. C) GFP Positive Clones also Show No Telomerase Activity in TRAP Assay. 2 of the 3 clones from the GFP negative population show telomerase activity despite having received a virus containing a gRNA directed to TERT.

Forward Genetic Screen Identifies ZNF827

Following our positive preliminary results, we decided to move forward in the design of our forward genetic screen. Each step in the process took many rounds of optimization to determine the optimal conditions for the screen. The overall flow for our final forward genetic screen is depicted in Figure 8A.

Our first attempt at a forward genetic screen was unsuccessful. We used the MT-hTR-AU5 virus cloned into a viral plasmid containing hygromycin resistance, however, the hygromycin selection was not completely effective which confounded our results. We also used the Human GeCKO CRISPR library A and library B, which was developed before current understanding of the rules that determine gRNA activity meaning that it is not as effective as more recently developed libraries (Doench et al., 2016a; Doench et al., 2014). Another difficulty in our first screen attempt was that we transduced the GeCKO libraries at an MOI 0.1 to ensure that each cell only got one gRNA and therefore only knocked out one gene. There are ~120,000 gRNAs in the combined GeCKO library so in order to have 100 fold representation of each gRNA and transduce at an MOI of 0.1 we had to begin the experiment with 120 million cells. In order to ensure that we maintained our library representation throughout the experiment we passaged a minimum of 16 million cells. Overall the first attempt was not successful and we did not see any likely candidate genes emerge from the sequencing results. Learning from this experience we decided to try again with many adjustments.

In our second screen we used the newer Human Brunello CRISPR knockout pooled library (Broad GPP), which was designed to be more effective than previous CRISPR libraries by following the recently developed gRNA design rules (Doench et al., 2016b; Doench et al., 2014). This time we also decided to transduce the cells with the Broad GPP library at an MOI of

3 which allowed us to passage fewer cells and through our analysis still determine which gRNAs were enriched. We again allowed the cells to grow for a few days following puromycin selection and then added the GFP expressing MT-hTR-AU5 at an MOI of 10, which was the MOI used for our preliminary studies. The cells were then plated lightly and allowed to grow for 15 days. In the past we showed that 15 days was sufficient to cause a significant reduction in transduced cells. At this point we sorted the cells into GFP positive and negative populations. We replated both populations and allowed the cells to grow for another 15 days. At this time, we collected genomic DNA from the GFP negative cells and resorted the GFP positive cells and collected genomic DNA directly from the GFP positive population following the sorting.

Once genomic DNA was collected, we performed two PCRs. The first PCR was used to amplify gRNAs and the second PCR was used to add illumina bar codes and adapters to the PCR products from the first PCR. The DNA from the GFP negative population received a different barcode from the DNA from the GFP positive population so that we could compare the results after sequencing. Afterwards qPCR was performed in order to determine accurate concentrations of DNA in each of the barcodes. All of the barcodes were then mixed and qPCR performed again to ensure the concentration of DNA was correct for deep sequencing. The samples were run on an illumina miseq at John Hopkin's University.

The results from the deep sequencing were split into barcodes using custom Pearl script, then the gRNA sequences were aligned to genes through Bowtie, and the results were analyzed through MaGeCK. We looked for gRNAs that were significantly enriched in the GFP positive group when compared to the GFP negative group. We also took into account how many gRNAs to the gene were found to be enriched. The GPP library has 4 gRNAs to each of the genes included in the library, so when more of the gRNAs are found to be enriched in the treatment

group, the more likely that candidate gene is to be a real hit. MaGeCK takes all of that information into account and ranks the genes in order of their positive selection score. The top 7 candidate genes can be seen in table 2. A gene enrichment plot for all of the genes included in the study is also shown in Figure 8B. The top 7 genes are indicated on the plot and their relation to the rest of the candidate genes can be seen.

From the results of this screen we decided to focus on the genes that had more than one gRNA enriched in the treatment sample as that increases the likelihood that the gene is a real hit. Of the top 7 genes, ZNF827, TMEM8C, GAD2, and OMG all had 3 gRNAs enriched in the treatment group. These 4 genes were all potential genes of interest, however, we decided to first focus on ZNF827. Not only was ZNF827 the top hit from the screen, but it has also been localized to the telomere (Conomos et al., 2014).

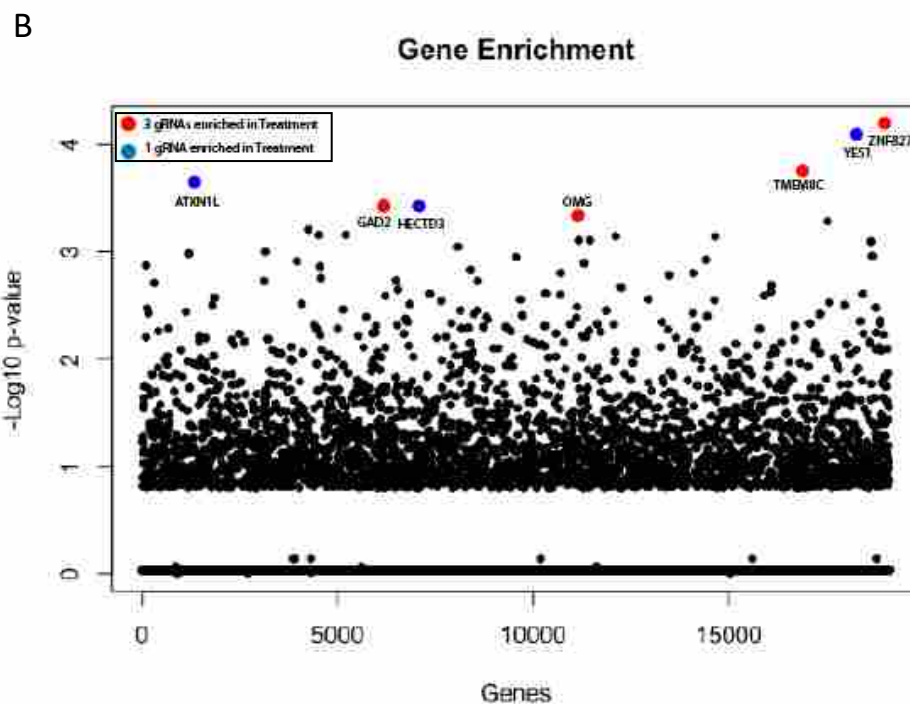
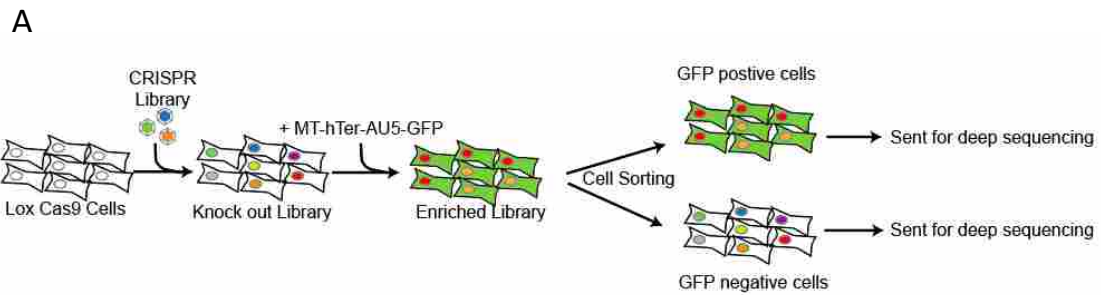


Figure 8: Forward Genetic Screen Experimental Design and Results. A) The Overall Flow of the Forward Genetic Xscreen. Cells are first transduced with the CRISPR library. Flowing selection cells are then transduced with MT-hTR-AU5 and allowed to grow for 15 days before sorting. The GFP positive cells were actually grown for another 15 days and resorted. Genomic DNA was then collected from the cells and sent for deep sequencing. B) Gene Ranking Shown as the $-\text{Log}_{10}$ p-value of the Positive P-value Score Calculated by MaGeCK. The genes that had 3 gRNAs enriched in the treatment group are shown in red. The genes that only had 1 gRNA enriched in the treatment group are shown in blue.

Table 2: Top Positive Ranked Genes from Forward Genetic Screen

Gene	Positive Rank	P-value	Enriched gRNAS	Gene Function
ZNF827	1	6.50E-05	3	Zinc finger protein of unknown function
YES1	2	7.80E-05	1	Tyrosine kinase- proto-oncogene
TMEM8C	3	1.73E-04	3	Mediates myoblast fusion
ATXN1L	4	2.22E-04	1	Chromatin binding factor- represses notch signalling
GAD2	5	3.53E-04	3	Glutamic acid decarboxylase- autoantigen in insulin dependent diabetes
HECTD3	6	3.78E-04	1	Transfers ubiquitin to targeted substrate for degradation
OMG	7	4.45E-04	3	Cell adhesion molecule found in the brain

ZNF827 Verification

ZNF827 is a zinc finger nuclease with little known about its function (Conomos et al., 2014; Pickett and Reddel, 2015). It has been reported to be localized to the telomere and recruit NuRD in association with alternative lengthening of telomeres (Conomos et al., 2014; Pickett and Reddel, 2015). Mutations in ZNF827 have also appeared in multiple genome-wide association studies for various conditions, however, no causal link has ever been shown (Chambers et al., 2011; Jiang et al., 2015; Kim et al., 2011; Sio et al., 2017). Because it was the top hit in our forward genetic screen as well as its localization to telomeres this became our top gene moving forward.

In order to confirm that ZNF827 knockout would result in protection from the MT-hTR-AU5 virus, we cloned a gRNA directed to ZNF827 in to lentiviral plasmid. After transduction of

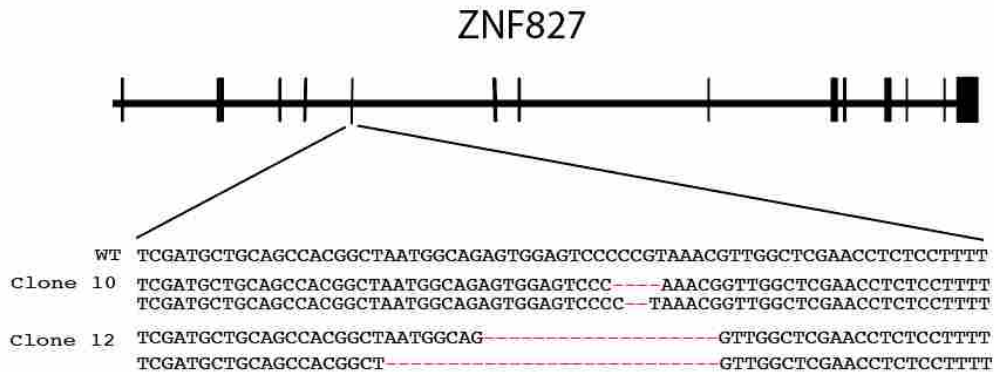
LOX Cas9 cells with the lentivirus containing the ZNF827 gRNA and selection with puromycin, we cloned the cell population to isolate a clone with confirmed knockout of ZNF827. In our screening we identified two clones (clone 10 and clone 12) that had deleterious mutations in both alleles of *ZNF827* (Figure 9A).

In order to test the resistance of ZNF827 knockout cells to the MT-hTR-AU5 virus, we again transduced LOX cells, TERT knockout LOX cells, and the ZNF827 knockout LOX cells with MT-hTR-AU5. We performed the transduction in triplicate and measured the GFP percentage through flow cytometry (Figure 9B). As expected, approximately two weeks after transduction, the wild type LOX cells had a low percentage of GFP positive cells remaining (Figure 9B). Unexpectedly, TERT knockout LOX cells also had a reduced number of GFP positive cells (Figure 9B). New TERT knockout cells have to be generated before each trial because cells have a limited number of divisions after knockout of telomerase function. During this knockout of TERT and selection there may have been a lower percentage of cells that fully disrupted telomerase function. We previously showed that some cells retained telomerase activity after transduction of the gRNA to TERT indicating that a portion of cells in this population may have had telomerase function

LOX ZNF827 knockout clone 10 showed significantly higher GFP percentages than wild type LOX cells at 6, 9, and 13 days post-transduction. The cells from this population appear to have some level of resistance to the MT-hTR-AU5 virus indicating that the knockout of ZNF827 is preventing the addition of mutant telomere sequence. However, LOX ZNF827 knockout clone 12 showed little resistance to MT-hTR-AU5 and only showed a significance difference from the control cells on day 6. Clone 12 sequencing results showed two mutations one of which was a 27bp deletion. This is a large deletion and so we initially assumed there would be no ZNF827

activity, however, since that is an in frame deletion there is a chance that these cells retained some ZNF827 activity, which may explain the different results between the two ZNF827 knockout clones.

A



B

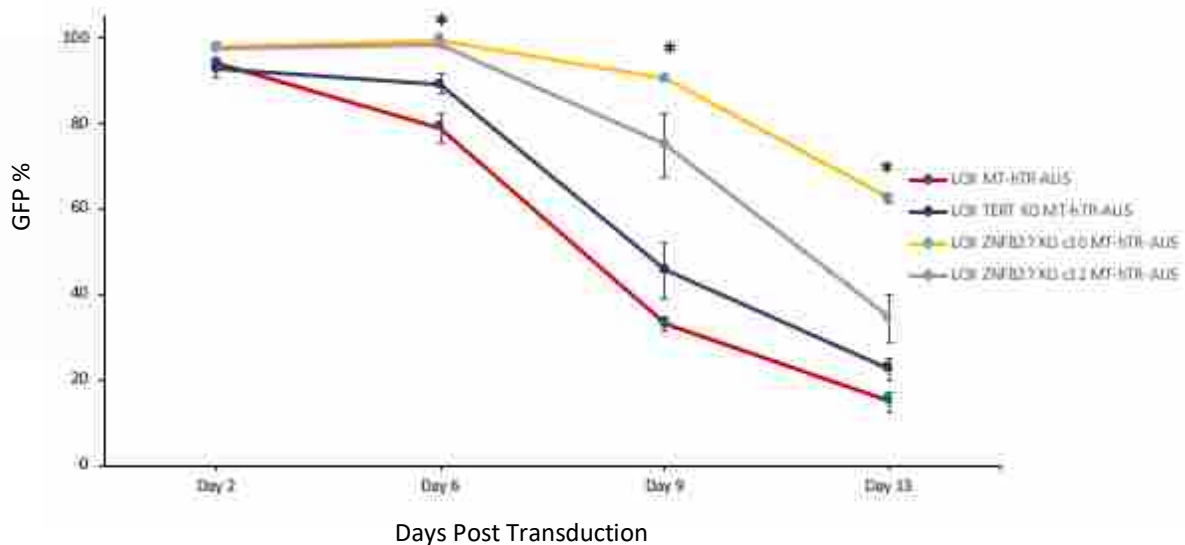


Figure 9: Verification of ZNF827. A) Sequencing Results From Two Isolated Clones. Both clones showed deleterious mutations in both alleles. B) Graph Showing Results of MT-hTR-AU5 transduction of Wild Type LOX cells, TERT KO LOX cells, and two ZNF827 KO LOX clones. ZNF827 KO clone 10 showed significant differences in GFP percentage from wild type LOX cells on days 6, 9, and 13 (p-values: 0.0025913, 0.0007739, 0.0004214 respectively). ZNF827 KO clone 12 only showed a significant difference from wild type LOX cells on day 6 (p value: 0.0034659).

DISCUSSION

The use of CRISPR-Cas9 for genome editing in laboratory settings has become an invaluable tool. It can be used to knock-out genes, modify gene expression, perform forward genetic screens, knock-in exogenous DNA such as fluorescent tags or selectable markers, along with many other uses. However, there was a need for further optimization of delivery of Cas9 components to make it more widely available. Many of the techniques used to effectively introduce Cas9 components either require specialized equipment or have additional biosafety requirements. The optimization of CRISPR-Cas9 using lipid-mediated transfection methods to introduce Cas9 and a gRNA will allow for more widespread use of this valuable technique.

We found through our optimization that ribonucleoprotein (RNP) transfection was the most efficient method for gene knockout in our reporter system. RNP transfection worked well for knockout of TERT, however, it interestingly did not work for KEAP1 knockout. Recent studies have shown that the sequence of the gRNA can actually affect transcription and stability of gRNAs in cells (Haeussler et al., 2016; Moreno-Mateos et al., 2015). Therefore, KEAP1 gRNA may have been readily degraded when transfected in RNP form, however, when expressed from a plasmid with a strong U6 promoter there may have been enough gRNA to effectively cut KEAP1. This shows that although RNP transfection was effective, it may not work in every situation.

RNA only transfection into stably expressing Cas9 cells had highest knock-in percentage using our HEK 293 FlpIn Δ ATG EGFP reporter system, however, very few cells survived selection. Despite the high percentage of edited cells, this makes RNA only transfections less promising. RNP lipofection also had a high level of edited cells and many more cells survived selection making RNP transfection overall more efficient for knocking-in exogenous DNA.

RNP transfection also has many benefits that make the use of CRISPR-Cas9 more efficient. One preparation of Cas9 protein will provide enough protein for many transfections. Also gRNA can be transcribed in one day as opposed to the many days of cloning required to create plasmids. The gRNA can also be tested functionally *in vitro* prior to cell transfection increasing the likelihood that genome editing will be successful in cells. Finally, the half-life of donor DNA in cells is short, only 50-90 minutes, so delivering pre-assembled functional RNP will allow Cas9 to cut faster and increase the chances of homology directed repair using the donor DNA template (Lechardeur et al., 1999; Woolf et al., 1990).

Interestingly we found that the optimal amount of donor template for exogenous DNA insertion differed with the various methods of introducing Cas9 and gRNA. This variation in concentration may be due to the different methods of Cas9 expression. With plasmid transfections, genome editing cannot take place until Cas9 is transcribed and translated from the plasmid which may require higher levels of donor template to be co-transfected so it is not degraded by the time Cas9 is functional. On the other hand, RNP is preassembled and ready to cut the DNA at the time of transfection and therefore may not require as much repair template to be present. RNA only transfections seemed the most detrimental to cells and high levels of donor template also reduced cell viability post selection, which may explain the low repair template amount in RNA only transfections.

We also found that short homology arms could be used effectively in both single and double stranded repair templates even with large knock-ins. This is important because it can greatly reduce the cloning time and cost required to create repair templates. This confirms the findings of previously published papers using short homology arms for donor templates (Liang et al., 2017; Natsume et al., 2016; Song and Stieger, 2017). We further showed that double stranded

templates with short homology arms can be created through PCR using primers ordered that contain the homology arms and a plasmid that contains the exogenous DNA insert. This method of creating large donor templates is fast, inexpensive, and easy to perform. This optimization using widely available resources should make CRISPR/Cas9 genome editing more accessible to all labs.

The use of CRISPR-Cas9 in a forward genetic screen allowed us to identify new potential genes involved in the telomere length maintenance pathway. In recent years, mutations in telomere related genes have been shown to cause a spectrum of diseases called the telomere syndromes, with the most prevalent disease being pulmonary fibrosis (Alder et al., 2008; Alder et al., 2015; Armanios and Blackburn, 2012; Armanios et al., 2007). As more telomere genes are linked to pulmonary fibrosis the number of familial pulmonary fibrosis cases with diagnosed genetic causes has increased. Now 25% of familial pulmonary fibrosis cases have been linked to mutations in telomere related genes, however, more than half of familial pulmonary fibrosis cases still have an unknown genetic cause (Alder et al., 2011; Alder et al., 2015; Fingerlin et al., 2013; Hoffman et al., 2016; Kropski et al., 2016; Petrovski et al., 2017). There may be more telomere related gene mutations contributing to pulmonary fibrosis that have not yet been discovered.

We decided to perform a screen to identify new genes involved in the telomere length maintenance pathway. Finding new components of this pathway will lead to a better understanding of the molecular mechanisms of telomere lengthening and could potentially aid in diagnosis of patients with telomere syndromes as well as provide avenues for future research.

Our screen used the MT-hTR-AU5 virus, which is predicted to add the mutated telomere sequence “TATATA”, to screen for cell populations missing a necessary component of the

telomere length maintenance pathway (Stohr and Blackburn, 2008; Stohr et al., 2010). MT-hTR-AU5 causes cell senescence or apoptosis by compromising the binding of shelterin to the telomere and therefore initiating a DNA damage response within the cell. If the CRISPR library knocks out a gene essential to the addition of new telomeric sequence, the mutated telomere sequence will not be added to the end of the chromosome protecting the cell from a damage response and subsequent cell death.

Of the top 7 candidate genes from our screen, 4 genes had 3 gRNAs enriched in the treatment group and 3 genes only had 1 gRNA enriched. We therefore decided to focus on the genes with more than one gRNA enriched. Our main interest was the top ranked gene, ZNF827, which is a zinc finger protein. There is not much known about the function of ZNF827, however, a previous publication localized it to the telomere in conjunction with alternative lengthening of telomeres (Conomos et al., 2014). However, the enrichment of ZNF827 in the treatment group in our screen indicates that it may actually be playing a role telomere length maintenance.

In order to verify that ZNF827 could protect from MT-hTR-AU5 infection we created ZNF827 knockout cell lines in LOX cells and transduced with MT-hTR-AU5. LOX ZNF827 knockout clone 10 cells showed a significant increase in GFP percentage following transduction with MT-hTR-AU5. This indicates that knockout of ZNF827 is disrupting the telomere length maintenance pathway and allowing for cell survival following infection with a virus containing mutated telomerase RNA. Interestingly LOX ZNF827 knockout clone 12 did not show this same protection from MT-hTR-AU5 transduction. The sequencing results of clone 12 indicate that one allele contained a 27bp deletion, which is an in frame deletion. We assumed a deletion that large would disrupt ZNF827 function, however, the results of the experiment indicate that there may be different expression levels of ZNF827 in clone 10 and clone 12.

The finding that ZNF827 may be linked to telomere length maintenance holds enormous research potential. Further work needs to be done to elucidate the exact role ZNF827 plays at the telomere which will give a clearer understanding of how new telomere sequence is added. Future research also need to be done to investigate potential links between ZNF827 mutations and clinical manifestations such as telomere syndromes. Overall, these findings could have far reaching effects both in research and clinical applications.

REFERENCES

- Alder, J.K., J.J. Chen, L. Lancaster, S. Danoff, S.C. Su, J.D. Cogan, I. Vulto, M. Xie, X. Qi, R.M. Tuder, J.A. Phillips, 3rd, P.M. Lansdorp, J.E. Loyd, and M.Y. Armanios. 2008. Short telomeres are a risk factor for idiopathic pulmonary fibrosis. *Proc Natl Acad Sci U S A*. 105:13051-13056.
- Alder, J.K., J.D. Cogan, A.F. Brown, C.J. Anderson, W.E. Lawson, P.M. Lansdorp, J.A. Phillips, 3rd, J.E. Loyd, J.J. Chen, and M. Armanios. 2011. Ancestral mutation in telomerase causes defects in repeat addition processivity and manifests as familial pulmonary fibrosis. *PLoS Genet*. 7:e1001352.
- Alder, J.K., S.E. Stanley, C.L. Wagner, M. Hamilton, V.S. Hanumanthu, and M. Armanios. 2015. Exome Sequencing Identifies Mutant TINF2 in a Family With Pulmonary Fibrosis. *Chest*. 147:1361-1368.
- Armanios, M. 2009. Syndromes of telomere shortening. *Annu Rev Genomics Hum Genet*. 10:45-61.
- Armanios, M. 2012. Telomerase and idiopathic pulmonary fibrosis. *Mutat Res*. 730:52-58.
- Armanios, M., and E.H. Blackburn. 2012. The telomere syndromes. *Nat Rev Genet*. 13:693-704.
- Armanios, M., J.L. Chen, Y.P. Chang, R.A. Brodsky, A. Hawkins, C.A. Griffin, J.R. Eshleman, A.R. Cohen, A. Chakravarti, A. Hamosh, and C.W. Greider. 2005. Haploinsufficiency of telomerase reverse transcriptase leads to anticipation in autosomal dominant dyskeratosis congenita. *Proc Natl Acad Sci U S A*. 102:15960-15964.
- Armanios, M.Y., J.J. Chen, J.D. Cogan, J.K. Alder, R.G. Ingersoll, C. Markin, W.E. Lawson, M. Xie, I. Vulto, J.A. Phillips, 3rd, P.M. Lansdorp, C.W. Greider, and J.E. Loyd. 2007. Telomerase mutations in families with idiopathic pulmonary fibrosis. *N Engl J Med*. 356:1317-1326.
- Barbaro, P.M., D.S. Ziegler, and R.R. Reddel. 2016. The wide-ranging clinical implications of the short telomere syndromes. *Intern Med J*. 46:393-403.
- Bhaya, D., M. Davison, and R. Barrangou. 2011. CRISPR-Cas systems in bacteria and archaea: versatile small RNAs for adaptive defense and regulation. *Annu Rev Genet*. 45:273-297.
- Bialk, P., N. Rivera-Torres, B. Strouse, and E.B. Kmiec. 2015. Regulation of Gene Editing Activity Directed by Single-Stranded Oligonucleotides and CRISPR/Cas9 Systems. *Plos One*. 10:e0129308.
- Bialk, P., B. Sansbury, N. Rivera-Torres, K. Bloh, D. Man, and E.B. Kmiec. 2016. Analyses of point mutation repair and allelic heterogeneity generated by CRISPR/Cas9 and single-stranded DNA oligonucleotides. *Sci Rep*. 6:32681.

- Bibikova, M., D. Carroll, D.J. Segal, J.K. Trautman, J. Smith, Y.G. Kim, and S. Chandrasegaran. 2001. Stimulation of homologous recombination through targeted cleavage by chimeric nucleases. *Mol Cell Biol.* 21:289-297.
- Bisht, K., S. Grill, J. Graniel, and J. Nandakumar. 2017. A lentivirus-free inducible CRISPR-Cas9 system for efficient targeting of human genes. *Anal Biochem.* 530:40-49.
- Blackburn, E.H., C.W. Greider, E. Henderson, M.S. Lee, J. Shampay, and D. Shippen-Lentz. 1989. Recognition and elongation of telomeres by telomerase. *Genome.* 31:553-560.
- Borie, R., C. Kannengiesser, N. Nathan, L. Tabeze, P. Pradere, and B. Crestani. 2015. Familial pulmonary fibrosis. *Rev Mal Respir.* 32:413-434.
- Chambers, J.C., W. Zhang, J. Sehmi, X. Li, M.N. Wass, P. Van der Harst, H. Holm, S. Sanna, M. Kavousi, S.E. Baumeister, L.J. Coin, G. Deng, C. Gieger, N.L. Heard-Costa, J.J. Hottenga, B. Kuhnel, V. Kumar, V. Lagou, L. Liang, J. Luan, P.M. Vidal, I. Mateo Leach, P.F. O'Reilly, J.F. Peden, N. Rahmioglu, P. Soininen, E.K. Speliotes, X. Yuan, G. Thorleifsson, B.Z. Alizadeh, L.D. Atwood, I.B. Borecki, M.J. Brown, P. Charoen, F. Cucca, D. Das, E.J. de Geus, A.L. Dixon, A. Doring, G. Ehret, G.I. Eyjolfsson, M. Farrall, N.G. Forouhi, N. Friedrich, W. Goessling, D.F. Gudbjartsson, T.B. Harris, A.L. Hartikainen, S. Heath, G.M. Hirschfield, A. Hofman, G. Homuth, E. Hypponen, H.L. Janssen, T. Johnson, A.J. Kangas, I.P. Kema, J.P. Kuhn, S. Lai, M. Lathrop, M.M. Lerch, Y. Li, T.J. Liang, J.P. Lin, R.J. Loos, N.G. Martin, M.F. Moffatt, G.W. Montgomery, P.B. Munroe, K. Musunuru, Y. Nakamura, C.J. O'Donnell, I. Olafsson, B.W. Penninx, A. Pouta, B.P. Prins, I. Prokopenko, R. Puls, A. Ruukonen, M.J. Savolainen, D. Schlessinger, J.N. Schouten, U. Seedorf, S. Sen-Chowdhry, K.A. Siminovitch, J.H. Smit, T.D. Spector, W. Tan, T.M. Teslovich, T. Tukiainen, A.G. Uitterlinden, M.M. Van der Klauw, R.S. Vasan, C. Wallace, H. Wallaschofski, H.E. Wichmann, G. Willemsen, P. Wurtz, C. Xu, L.M. Yerges-Armstrong, et al. 2011. Genome-wide association study identifies loci influencing concentrations of liver enzymes in plasma. *Nat Genet.* 43:1131-1138.
- Chang, H.H.Y., N.R. Pannunzio, N. Adachi, and M.R. Lieber. 2017. Non-homologous DNA end joining and alternative pathways to double-strand break repair. *Nat Rev Mol Cell Biol.* 18:495-506.
- Chapman, J.R., M.R. Taylor, and S.J. Boulton. 2012. Playing the end game: DNA double-strand break repair pathway choice. *Mol Cell.* 47:497-510.
- Cong, L., F.A. Ran, D. Cox, S. Lin, R. Barretto, N. Habib, P.D. Hsu, X. Wu, W. Jiang, L.A. Marraffini, and F. Zhang. 2013. Multiplex genome engineering using CRISPR/Cas systems. *Science.* 339:819-823.
- Conomos, D., R.R. Reddel, and H.A. Pickett. 2014. NuRD-ZNF827 recruitment to telomeres creates a molecular scaffold for homologous recombination. *Nat Struct Mol Biol.* 21:760-770.

- Cronkhite, J.T., C. Xing, G. Raghu, K.M. Chin, F. Torres, R.L. Rosenblatt, and C.K. Garcia. 2008. Telomere shortening in familial and sporadic pulmonary fibrosis. *American journal of respiratory and critical care medicine*. 178:729-737.
- Dai, J., H. Cai, H. Li, Y. Zhuang, H. Min, Y. Wen, J. Yang, Q. Gao, Y. Shi, and L. Yi. 2015. Association between telomere length and survival in patients with idiopathic pulmonary fibrosis. *Respirology*. 20:947-952.
- de Lange, T. 2005. Shelterin: the protein complex that shapes and safeguards human telomeres. *Genes Dev*. 19:2100-2110.
- de Lange, T. 2010. How shelterin solves the telomere end-protection problem. *Cold Spring Harb Symp Quant Biol*. 75:167-177.
- Doench, J.G., N. Fusi, M. Sullender, M. Hegde, E.W. Vaimberg, K.F. Donovan, I. Smith, Z. Tothova, C. Wilen, R. Orchard, H.W. Virgin, J. Listgarten, and D.E. Root. 2016a. Optimized sgRNA design to maximize activity and minimize off-target effects of CRISPR-Cas9. *Nat Biotechnol*. 34:184-191.
- Doench, J.G., N. Fusi, M. Sullender, M. Hegde, E.W. Vaimberg, K.F. Donovan, I. Smith, Z. Tothova, C. Wilen, R. Orchard, H.W. Virgin, J. Listgarten, and D.E. Root. 2016b. Optimized sgRNA design to maximize activity and minimize off-target effects of CRISPR-Cas9. *Nat Biotechnol*. 34:184-191.
- Doench, J.G., E. Hartenian, D.B. Graham, Z. Tothova, M. Hegde, I. Smith, M. Sullender, B.L. Ebert, R.J. Xavier, and D.E. Root. 2014. Rational design of highly active sgRNAs for CRISPR-Cas9-mediated gene inactivation. *Nat Biotechnol*. 32:1262-1267.
- Doksani, Y., and T. de Lange. 2014. The role of double-strand break repair pathways at functional and dysfunctional telomeres. *Cold Spring Harb Perspect Biol*. 6:a016576.
- Dow, L.E., J. Fisher, K.P. O'Rourke, A. Muley, E.R. Kasthuber, G. Livshits, D.F. Tschaharganeh, N.D. Socci, and S.W. Lowe. 2015. Inducible in vivo genome editing with CRISPR-Cas9. *Nat Biotechnol*. 33:390-394.
- Fingerlin, T.E., E. Murphy, W. Zhang, A.L. Peljto, K.K. Brown, M.P. Steele, J.E. Loyd, G.P. Cosgrove, D. Lynch, S. Groshong, H.R. Collard, P.J. Wolters, W.Z. Bradford, K. Kossen, S.D. Seiwert, R.M. du Bois, C.K. Garcia, M.S. Devine, G. Gudmundsson, H.J. Isaksson, N. Kaminski, Y. Zhang, K.F. Gibson, L.H. Lancaster, J.D. Cogan, W.R. Mason, T.M. Maher, P.L. Molyneaux, A.U. Wells, M.F. Moffatt, M. Selman, A. Pardo, D.S. Kim, J.D. Crapo, B.J. Make, E.A. Regan, D.S. Walek, J.J. Daniel, Y. Kamatani, D. Zelenika, K. Smith, D. McKean, B.S. Pedersen, J. Talbert, R.N. Kidd, C.R. Markin, K.B. Beckman, M. Lathrop, M.I. Schwarz, and D.A. Schwartz. 2013. Genome-wide association study identifies multiple susceptibility loci for pulmonary fibrosis. *Nat Genet*. 45:613-620.
- Gagnon, J.A., E. Valen, S.B. Thyme, P. Huang, L. Akhmetova, A. Pauli, T.G. Montague, S. Zimmerman, C. Richter, and A.F. Schier. 2014. Efficient mutagenesis by Cas9 protein-

- mediated oligonucleotide insertion and large-scale assessment of single-guide RNAs. *PLoS One*. 9:e98186.
- Goldkorn, A., and E.H. Blackburn. 2006. Assembly of mutant-template telomerase RNA into catalytically active telomerase ribonucleoprotein that can act on telomeres is required for apoptosis and cell cycle arrest in human cancer cells. *Cancer Res*. 66:5763-5771.
- Greider, C.W., and E.H. Blackburn. 1985. Identification of a specific telomere terminal transferase activity in Tetrahymena extracts. *Cell*. 43:405-413.
- Haeussler, M., K. Schonig, H. Eckert, A. Eschstruth, J. Mianne, J.B. Renaud, S. Schneider-Maunoury, A. Shkumatava, L. Teboul, J. Kent, J.S. Joly, and J.P. Concordet. 2016. Evaluation of off-target and on-target scoring algorithms and integration into the guide RNA selection tool CRISPOR. *Genome Biol*. 17:148.
- Hayes, J.D., and M. McMahon. 2001. Molecular basis for the contribution of the antioxidant responsive element to cancer chemoprevention. *Cancer Lett*. 174:103-113.
- Hoffman, T.W., J.J. van der Vis, M.F. van Oosterhout, H.W. van Es, D.A. van Kessel, J.C. Grutters, and C.H. van Moorsel. 2016. TINF2 Gene Mutation in a Patient with Pulmonary Fibrosis. *Case Rep Pulmonol*. 2016:1310862.
- Hutchinson, J., A. Fogarty, R. Hubbard, and T. McKeever. 2015. Global incidence and mortality of idiopathic pulmonary fibrosis: a systematic review. *Eur Respir J*. 46:795-806.
- Hutchinson, J.P., T.M. McKeever, A.W. Fogarty, V. Navaratnam, and R.B. Hubbard. 2014. Increasing global mortality from idiopathic pulmonary fibrosis in the twenty-first century. *Ann Am Thorac Soc*. 11:1176-1185.
- Jasin, M., and R. Rothstein. 2013. Repair of strand breaks by homologous recombination. *Cold Spring Harb Perspect Biol*. 5:a012740.
- Jiang, S., W. Yang, Y. Qiu, H.Z. Chen, and I. Alzheimer's Disease Neuroimaging. 2015. Identification of novel quantitative traits-associated susceptibility loci for APOE epsilon 4 non-carriers of Alzheimer's disease. *Curr Alzheimer Res*. 12:218-227.
- Jinek, M., K. Chylinski, I. Fonfara, M. Hauer, J.A. Doudna, and E. Charpentier. 2012. A programmable dual-RNA-guided DNA endonuclease in adaptive bacterial immunity. *Science*. 337:816-821.
- Katoh, Y., K. Iida, M.I. Kang, A. Kobayashi, M. Mizukami, K.I. Tong, M. McMahon, J.D. Hayes, K. Itoh, and M. Yamamoto. 2005. Evolutionary conserved N-terminal domain of Nrf2 is essential for the Keap1-mediated degradation of the protein by proteasome. *Arch Biochem Biophys*. 433:342-350.
- Kim, S., D. Kim, S.W. Cho, J. Kim, and J.S. Kim. 2014. Highly efficient RNA-guided genome editing in human cells via delivery of purified Cas9 ribonucleoproteins. *Genome Res*. 24:1012-1019.

- Kim, Y.J., M.J. Go, C. Hu, C.B. Hong, Y.K. Kim, J.Y. Lee, J.Y. Hwang, J.H. Oh, D.J. Kim, N.H. Kim, S. Kim, E.J. Hong, J.H. Kim, H. Min, Y. Kim, R. Zhang, W. Jia, Y. Okada, A. Takahashi, M. Kubo, T. Tanaka, N. Kamatani, K. Matsuda, M. consortium, T. Park, B. Oh, K. Kimm, D. Kang, C. Shin, N.H. Cho, H.L. Kim, B.G. Han, J.Y. Lee, and Y.S. Cho. 2011. Large-scale genome-wide association studies in East Asians identify new genetic loci influencing metabolic traits. *Nat Genet.* 43:990-995.
- Kropski, J.A., L.R. Young, J.D. Cogan, D.B. Mitchell, L.H. Lancaster, J.A. Worrell, C. Markin, N. Liu, W.R. Mason, T.E. Fingerlin, D.A. Schwartz, W.E. Lawson, T.S. Blackwell, J.A. Phillips Iii, and J.E. Loyd. 2016. Genetic Evaluation and Testing of Patients and Families with Idiopathic Pulmonary Fibrosis. *American journal of respiratory and critical care medicine.*
- Lackner, D.H., D. Durocher, and J. Karlseder. 2011. A siRNA-based screen for genes involved in chromosome end protection. *Plos One.* 6:e21407.
- Lechardeur, D., K.J. Sohn, M. Haardt, P.B. Joshi, M. Monck, R.W. Graham, B. Beatty, J. Squire, H. O'Brodovich, and G.L. Lukacs. 1999. Metabolic instability of plasmid DNA in the cytosol: a potential barrier to gene transfer. *Gene Ther.* 6:482-497.
- Liang, X., J. Potter, S. Kumar, N. Ravinder, and J.D. Chesnut. 2017. Enhanced CRISPR/Cas9-mediated precise genome editing by improved design and delivery of gRNA, Cas9 nuclease, and donor DNA. *J Biotechnol.* 241:136-146.
- Lin, S., B.T. Staahl, R.K. Alla, and J.A. Doudna. 2014. Enhanced homology-directed human genome engineering by controlled timing of CRISPR/Cas9 delivery. *Elife.* 3:e04766.
- Makarova, K.S., Y.I. Wolf, O.S. Alkhnbashi, F. Costa, S.A. Shah, S.J. Saunders, R. Barrangou, S.J. Brouns, E. Charpentier, D.H. Haft, P. Horvath, S. Moineau, F.J. Mojica, R.M. Terns, M.P. Terns, M.F. White, A.F. Yakunin, R.A. Garrett, J. van der Oost, R. Backofen, and E.V. Koonin. 2015. An updated evolutionary classification of CRISPR-Cas systems. *Nat Rev Microbiol.* 13:722-736.
- Mali, P., L. Yang, K.M. Esvelt, J. Aach, M. Guell, J.E. DiCarlo, J.E. Norville, and G.M. Church. 2013. RNA-guided human genome engineering via Cas9. *Science.* 339:823-826.
- Martinez, P., and M.A. Blasco. 2017. Telomere-driven diseases and telomere-targeting therapies. *J Cell Biol.* 216:875-887.
- Mender, I., and J.W. Shay. 2015. Telomerase Repeated Amplification Protocol (TRAP). *Bio Protoc.* 5.
- Moreno-Mateos, M.A., C.E. Vejnar, J.D. Beaudoin, J.P. Fernandez, E.K. Mis, M.K. Khokha, and A.J. Giraldez. 2015. CRISPRscan: designing highly efficient sgRNAs for CRISPR-Cas9 targeting in vivo. *Nat Methods.* 12:982-988.

- Moyer, T.C., and A.J. Holland. 2015. Generation of a conditional analog-sensitive kinase in human cells using CRISPR/Cas9-mediated genome engineering. *Methods Cell Biol.* 129:19-36.
- Natsume, T., T. Kiyomitsu, Y. Saga, and M.T. Kanemaki. 2016. Rapid Protein Depletion in Human Cells by Auxin-Inducible Degron Tagging with Short Homology Donors. *Cell Rep.* 15:210-218.
- Newton, C.A., J. Kozlitina, J.R. Lines, V. Kaza, F. Torres, and C.K. Garcia. 2017. Telomere length in patients with pulmonary fibrosis associated with chronic lung allograft dysfunction and post-lung transplantation survival. *J Heart Lung Transplant.* 36:845-853.
- Petrovski, S., J.L. Todd, M.T. Durheim, Q. Wang, J.W. Chien, F.L. Kelly, C. Frankel, C.M. Mebane, Z. Ren, J. Bridgers, T.J. Urban, C.D. Malone, A. Finlen Copeland, C. Brinkley, A.S. Allen, T. O'Riordan, J.G. McHutchison, S.M. Palmer, and D.B. Goldstein. 2017. An Exome Sequencing Study to Assess the Role of Rare Genetic Variation in Pulmonary Fibrosis. *American journal of respiratory and critical care medicine.* 196:82-93.
- Pickett, H.A., and R.R. Reddel. 2015. Molecular mechanisms of activity and derepression of alternative lengthening of telomeres. *Nat Struct Mol Biol.* 22:875-880.
- Planas, L., E.G. Arias-Salgado, I.B. Roldan, A. Montes, C. Esquinas, V.V. Zygmunt, P. Luburich, R. Llatjos, C. Machahua, P. Rivera, L. Pintado-Berninches, V. Leiro, E. Balcells, E. Sala, J. Cortijo, J. Dorca, R. Perona, M. Selman, and M. Molina-Molina. 2017. Clinical Predictive Factors And Prognostic Implications Of Telomere Shortening In Sporadic And Familial Idiopathic Pulmonary Fibrosis. *American journal of respiratory and critical care medicine.* 195.
- Ran, F.A., P.D. Hsu, J. Wright, V. Agarwala, D.A. Scott, and F. Zhang. 2013. Genome engineering using the CRISPR-Cas9 system. *Nat Protoc.* 8:2281-2308.
- Richardson, C.D., G.J. Ray, M.A. DeWitt, G.L. Curie, and J.E. Corn. 2016. Enhancing homology-directed genome editing by catalytically active and inactive CRISPR-Cas9 using asymmetric donor DNA. *Nat Biotechnol.* 34:339-344.
- Rivera-Torres, N., K. Banas, P. Bialk, K.M. Bloh, and E.B. Kmiec. 2017. Insertional Mutagenesis by CRISPR/Cas9 Ribonucleoprotein Gene Editing in Cells Targeted for Point Mutation Repair Directed by Short Single-Stranded DNA Oligonucleotides. *Plos One.* 12:e0169350.
- Sander, J.D., and J.K. Joung. 2014. CRISPR-Cas systems for editing, regulating and targeting genomes. *Nat Biotechnol.* 32:347-355.
- Sanjana, N.E., O. Shalem, and F. Zhang. 2014. Improved vectors and genome-wide libraries for CRISPR screening. *Nat Methods.* 11:783-784.
- Schmidt, J.C., and T.R. Cech. 2015. Human telomerase: biogenesis, trafficking, recruitment, and activation. *Genes Dev.* 29:1095-1105.

- Sihvola, V., and A.L. Levonen. 2017. Keap1 as the redox sensor of the antioxidant response. *Arch Biochem Biophys.* 617:94-100.
- Sio, C.A., K. Jung, J.H. Kim, H.S. Cheong, E. Shin, H. Jang, M. Yoon, H. Jang, and H.D. Shin. 2017. Sotos syndrome associated with Hirschsprung's disease: a new case and exome-sequencing analysis. *Pediatr Res.* 82:87-92.
- Song, F., and K. Stieger. 2017. Optimizing the DNA Donor Template for Homology-Directed Repair of Double-Strand Breaks. *Mol Ther Nucleic Acids.* 7:53-60.
- Stanley, S.E., D.L. Gable, C.L. Wagner, T.M. Carlile, V.S. Hanumanthu, J.D. Podlevsky, S.E. Khalil, A.E. DeZern, M.F. Rojas-Duran, C.D. Applegate, J.K. Alder, E.M. Parry, W.V. Gilbert, and M. Armanios. 2016. Loss-of-function mutations in the RNA biogenesis factor NAF1 predispose to pulmonary fibrosis-emphysema. *Sci Transl Med.* 8:351ra107.
- Stohr, B.A., and E.H. Blackburn. 2008. ATM mediates cytotoxicity of a mutant telomerase RNA in human cancer cells. *Cancer Res.* 68:5309-5317.
- Stohr, B.A., L. Xu, and E.H. Blackburn. 2010. The terminal telomeric DNA sequence determines the mechanism of dysfunctional telomere fusion. *Mol Cell.* 39:307-314.
- Stuart, B.D., J. Choi, S. Zaidi, C. Xing, B. Holohan, R. Chen, M. Choi, P. Dharwadkar, F. Torres, C.E. Girod, J. Weissler, J. Fitzgerald, C. Kershaw, J. Klesney-Tait, Y. Mageto, J.W. Shay, W. Ji, K. Bilguvar, S. Mane, R.P. Lifton, and C.K. Garcia. 2015. Exome sequencing links mutations in PARN and RTEL1 with familial pulmonary fibrosis and telomere shortening. *Nat Genet.* 47:512-517.
- van de Loosdrecht, A.A., R.H. Beelen, G.J. Ossenkoppele, M.G. Broekhoven, and M.M. Langenhuijsen. 1994. A tetrazolium-based colorimetric MTT assay to quantitate human monocyte mediated cytotoxicity against leukemic cells from cell lines and patients with acute myeloid leukemia. *J Immunol Methods.* 174:311-320.
- Woolf, T.M., C.G. Jennings, M. Rebagliati, and D.A. Melton. 1990. The stability, toxicity and effectiveness of unmodified and phosphorothioate antisense oligodeoxynucleotides in *Xenopus* oocytes and embryos. *Nucleic Acids Res.* 18:1763-1769.

Table S1: Supplemental Table of Primers Oligonucleotides Used for Screening and Cloning.

Primers for Double Stranded Repair Templates	Sequence (5'-3')	Description
TagRFP_knockin_Fwd	AAGCTTGGTACCGAGCTCGGATCC GCCACC ATGGTGTCTAAGGGCGAAGAG	Template for RFP-linker knock-in with 35bp homology arms
TagRFP_knockin_Rev2	CCCGGTGAACAGCTCCTCGCCCTTGTCTAC GCCAGAGCCGCCGCC	
Primers for IVT template	Sequence (5'-3')	Description
T7_GFP_sgRNA_1	TGTAATACGACTCACTATAGGGGCGAGGAGCTGTTACCGGTTTTAGAGCTAG AAATAGC	gRNA used for GFP knock out
T7_GFP_sgRNA_3	TGTAATACGACTCACTATAGGGATCCGCCACCGTGAGCAAGTTTTAGAGCTAG AAATAGC	gRNA used for ΔATG-EGFP cutting and knock-in
T7_hTERT-RT_sgRNA	TGTAATACGACTCACTATAGGGCCAGGGCCTCGTCTTCTACAGTTTTAGAGCTA GAAATAGC	gRNA used for hTERT knock out
T7_KEAP1_sgRNA	TGTAATACGACTCACTATAGGGCCGAGCCCGTTGGTGAACAGTTTTAGAGCT AGAAATAGC	gRNA used to try RNP knock out of Keap1
sgRNA_Rev	AAAAAAGCACCGACTCGGTGCCACT	
Oligos for px459v2 plasmid construction	Sequence (5'-3')	Description
GFP_sgRNA_1_top	CACCGGGGCGAGGAGCTGTTACCG	Ligated into px459v2
GFP_sgRNA_1_bottom	AAACCGGTGAACAGCTCCTCGCCCC	
GFP_sgRNA_2_top	CACCGCAGCTCCTCGCCCTTGCTCA	
GFP_sgRNA_2_bottom	AAACTGAGCAAGGGGCGAGGAGCTGC	
Keap1_CRISPR_top	CACCGCCGAGCCCGTTGGTGA	
Keap1_CRISPR_bottom	AAACTGTTACCAACGGGCTGC	
Single Stranded Repair Templates	Sequence (5'-3')	Description
GFP_ssRepair30	AAGCTTGGTACCGAGCTCGGATCCGCCACCATGGTGAGCAAGGGGCGAGGAGC TGTTACCGGG	ATG only repair template with 30bp homology arms
deltaATG_GFP_FLAG_ssdonor	AAGCTTGGTACCGAGCTCGGATCCGCCACCATGGATTACAAAGACGATGACGA TAAGGTGAGCAAGGGGCGAGGAGCTGTTACCGGG	FLAG-ATG repair template with 30bp homology arms.
Screening Primers	Sequence (5'-3')	Description
hTERT_seq_fwd1.1	GCGTGCCTGGGACG	For hTERT knock out screening
hTERT_seq_Rev1	TATGGTTCAGGCCCGTTCCG	
Keap1_scrn_fwd1	TTGGCATCATGAACGAGCTG	
Keap1_scrn_rev1	TAGGCGAATTCAATGAGGCG	
		For Keap1 knock out screening

CURRICULUM VITAE

Kelsey Phillips

535 N 800 E, Provo, UT 84606

916-698-8796

Kelsey.ringer@gmail.com

EDUCATION

Brigham Young University, Provo, UT
Masters Student 2015 - 2018
Thesis: CRISPR-Cas9 Transfection Optimization and use in Forward Genetic Screen to Identify Telomere Length Maintenance Genes
Mentors: Dr. Jonathan Alder and Dr. Jason Hansen

Brigham Young University, Provo, UT
B.S. in Physiology and Developmental Biology 2007 - 2011
Minor in Chemistry

AWARDS

Research Assistantship	January 2016 – January 2018
Teaching Assistantship	August 2015 – January 2018
Tuition Awards	August 2015-August 2017
PDBio Graduate Retreat: 1 st Place Oral Presentation	January 2017
Simmons Center Cancer Research Fellowship	January 2016
Magnum Cum Laude Graduate – Undergraduate Degree	January 2011
Gordon B. Hinckley Presidential Scholarship	January 2007 – January 2011

WORK EXPERIENCE

Brigham Young University
Research Assistant 2016-2018

- Roles included cell culture, animal care, and molecular biology techniques

Teaching Assistant 2015-2018

- Courses included Human Physiology, Advanced Physiology Lab, and Developmental Biology.
- Roles, for all classes, included grading papers, answering student questions and reviewing content during office hours and periodic reviews and lab sessions
- Taught classes when professors were unavailable

Kaplan Test Prep MCAT Instructor, Tutor, and Mentor	2012-2016
<ul style="list-style-type: none"> • Taught science content and test strategies to hundreds of pre-medical students in classroom settings • Mentored new teachers to help them master content and teaching skills 	
GRE Instructor	2014-2015
<ul style="list-style-type: none"> • Used my experience from taking the GRE to mentor students preparing for graduate school. • Taught test strategies and reviewed content. 	
ACT and SAT Instructor and Tutor	2013-2015
<ul style="list-style-type: none"> • Helped students prepared for the ACT and SAT through guided instruction of test strategies. • Worked with many students in one-on-one tutoring sessions 	

RESEARCH EXPERIENCE

Brigham Young University- Dr. Hansen's Lab	2017-2018
<ul style="list-style-type: none"> • Assisted with cell culture techniques including, CRISPR-Cas9 knockout, viral packaging, and transfection 	
Dr. Alder's Lab	2015-2017
<ul style="list-style-type: none"> • Studied the role of telomeres in pulmonary fibrosis and cancer • Optimized use of CRISPR/Cas9 for genome editing in cell culture • Mastered cell culture techniques including a forward genetic screen in cells, viral packaging, and transfection • Used many molecular biology techniques in the lab 	
Dr. Hansen's Lab	2015
<ul style="list-style-type: none"> • Studied the role of Nrf2 in mediating resistance to oxidative stress in developing embryos • Used whole embryo culture to study the effect of Nrf2 inducers 	
Dr. Edward's Lab	2010 – 2011
<ul style="list-style-type: none"> • Performed single cell RT-qPCR on neurons collected from rat brains exposed to nicotine and alcohol to look for variation in nicotinic receptors. 	

PUBLICATIONS

Comparative Analysis of Lipid-Mediated CRISPR-Cas9 Genome Editing Techniques

Ringer K.P., Roth, M.G., Garey, M.S., Piorczynski, T.B., Suli, A, Hansen, J.M., Alder, J.K.
2018

Nrf2 Activation Prevents Valproic Acid-induced Redox Imbalance and Malformation in
Mouse Embryos

Harris, C., Jilek J. L., Sant, K., Ringer, K.P., Stucki, D. and Hansen J.M.
In preparation